classification subgroups. As tumor phenotype likely reflects underlying genetic alterations, direct molecular study of these alterations may be beneficial in understanding not only the morphological but also the biological potential of tumors.

In this study, useful genes possessing the ability to predict early intrahepatic recurrence of HCC were selected by gene expression profile analysis of 60 patients using a PCR-based array system; the usefulness of this technique for future clinical applications was estimated by comparison with other conventional indicators in a validation group composed of additional 40 patients.

2. Materials and methods

2.1. Tissues and patients

After obtaining informed consent, liver tissue specimens and clinical data were acquired from 60 patients who underwent hepatic resection for HCC at Osaka University Hospital between January 1997 and October 1999. The selection criteria applied for HCC resection in our hospital were the limitation of the area of spreading tumor(s) to two segments of the liver and the absence of distant metastases (M0). However, when we found small tumor(s) just outside of the resection area by intraoperative US, we resected all tumors if possible. All patients in the estimation group had no visible tumor after surgery and were followed for tumor recurrence in the liver at least every 3 months by identification of tumor markers and imaging modalities. The onset of tumor recurrence was designated as the time at which the tumor was detected by one of these imaging techniques; tumor recurrence was confirmed by surgical resection or hepatic angiography. The median follow-up time for patients in the estimation group was 51 months overall. To select informative genes for prediction of early recurrence, patients were divided into two groups: a recurrence group ($n = 32$), in which reappearance of disease was observed in the remnant liver within two years of surgery, and a recurrence-free group ($n = 28$), lacking any observable disease at more than two years after primary surgery. As a validation group, we have collected liver tissue specimens and clinical data from 40 additional HCC patients who underwent hepatic resection after November 1999. The selection criteria and the method of follow-up in the validation group were as same as those in the estimation group. The median follow-up time in the validation group was 40 months. All aspects of our study protocol were approved by the ethics committee of Osaka University.

2.2. PCR-based array system

To select genes expressed in liver tissues, we constructed three cDNA libraries from a mixture of HCC and non-tumorous livers, from normal livers, and from metastatic liver cancers, as described [8]. To construct the HCC library, a mixture of total RNAs from more than 10 HCC liver tissues were used; 2673 unique sequences were obtained from 9600 clones. We could design PCR primers for adaptor-tagged competitive PCR (ATAC-PCR) reactions for a total of 2384 genes from this EST collection. We prepared 130 primers from the normal liver library and 260 primers from the metastatic liver cancer library. In total, we prepared 3072 primers for ATAC-PCR, which included an additional 298 genes established in previous literature. The specificity of this gene selection provides an advantage over more universal sets, such as those selected from the UniGene database, which include genes not expressed in liver tissues. The ATAC-PCR experimental procedure was performed as described [9–14].

2.3. Analysis of PCR-based array data

The relative expression level of each gene was calculated by calibration using a standard mixture of more than 20 liver tissues including HCC and non-tumorous samples, as described [11–14]. Expression levels below 0.05 were regarded as missing values, likely resulting from noise. As strict filtering, we selected only 1546 genes which included fewer missing values. Following conversion to a logarithmic scale (base 2), the data matrix was normalized to a mean of 0 by standardizing each sample.

Permutation testing, which involves randomly permuting class labels to determine gene–class correlations [15–18], was used to select candidates for predictive genes from the estimation group. As a supervised classification method using the selected genes from the permutation test, we adopted a weighted voting (WV) algorithm, generally used in gene expression profiling [15–19]. Briefly, we calculated the signal-to-noise ratio, $S_i = (\mu_A - \mu_B)/(\sigma_A + \sigma_B)$, where μ and σ represent the mean and standard deviation of expression for each class, respectively. Each gene, g_i, is classified into either class A or class B depending on whether the expression level, X_i, in the test sample is closer to the mean expression level of class A (μ_A) or class B (μ_B) genes in the training samples. The magnitude of this vote (v_i) reflects the deviation of the test sample X_i value from the average of the two classes: $v_i = S_i(X_i - (\mu_A + \mu_B)/2)$. We summed the v_i values to obtain the total votes for class A (V_A) and class B (V_B) sub-classifications. The prediction strength is $(V_A - |V_B|)/(V_A + |V_B|)$, and we adopted the threshold as 0. If the strength is a positive number, we determine that the test sample belongs to class A. If the strength is a negative number, the test sample belongs to class B. This model was evaluated by leave-one-out cross-validation [15–20].

Hierarchical cluster analysis using a complete linkage method with Pearson's correlation was performed using GeneMaths 2.0 software. Other statistical analyses were performed using StatView 5.0J software. Correlations between intrahepatic recurrence and clinicopathological parameters were evaluated by both the χ^2 test with Yates correction and the log-rank test. Probability of recurrence curves and overall survival curves were calculated with the Kaplan–Meier method. Every log-rank test and a multivariate Cox analysis were performed with the time to intrahepatic recurrence except for overall survival analysis. The presence of a statistically significant difference was denoted by $P < 0.05$. Supplementary information including the list of examined genes is available on our web site (http://love2.aist-nara.ac.jp/laboratory/index_frame.html).

3. Results

3.1. Characteristics of the estimation group

In the estimation group, the clinicopathological characteristics of the recurrence group and the recurrence-free group were compared by the χ^2 test (Table 1). Significant differences were observed in tumor size ($P = 0.037$), tumor multiplicity ($P = 0.002$), and microscopic vascular invasion ($P = 0.035$), all of which are included within the conventional prognostic indicator, UICC TNM staging [21].

Next, to analyze also the correlations between base-line variables and the probability of intrahepatic recurrence, we performed a univariate analysis of patients in the estimation group with the log-rank test (Table 2). Patients with solitary tumors had a significantly lower recurrence rate than those with multiple tumors ($P < 0.001$). The absence of microscopic vascular invasion was also a significant factor for recurrence ($P = 0.003$). There were no significant differences in other factors that could be associated with the intrahepatic recurrence rate.

3.2. Selection of genes predicting early intrahepatic recurrence

In the estimation group ($n = 60$), permutation testing with 50,000 random trials selected 92 significant genes

Table 1
Clinicopathological characteristics between recurrence cases and recurrence-free cases in the estimation group

Parameters		Recurrence cases ($n = 32$)	Recurrence-free cases ($n = 28$)	P value[b]
Age (years)	<65 years	19	11	0.196
	≥65 years	13	17	
Sex	Male	25	23	0.948
	Female	7	5	
HBs Ag	Negative	26	26	0.348
	Positive	6	2	
HCV Ab	Negative	9	10	0.725
	Positive	23	18	
Child grade	A	22	20	> 0.999
	B	10	8	
Liver cirrhosis	Absent	15	12	0.959
	Present	17	16	
AFP	<100 ng/ml	14	20	0.058
	≥100 ng/ml	18	8	
Preoperative TAE	Not performed	24	21	> 0.999
	Performed	8	7	
Surgical margin	Negative	9	8	> 0.999
	Positive	23	20	
Histological grade[a]	Wel	2	3	0.807
	Mod	16	14	
	Por	14	11	
Tumor size	≤2 cm	4	11	0.037
	>2 cm	28	17	
Tumor multiplicity	Solitary	14	24	0.002
	Multiple	18	4	
Microscopic vascular invasion	Absent	17	23	0.035
	Present	15	5	
Lymph node metastasis	Absent	32	27	0.946
	Present	0	1	
Adjuvant therapy	Not performed	28	27	0.435
	Performed	4	1	

[a] Histological degree of HCC; wel, well differentiated; mod, moderately differentiated; por, poorly differentiated.
[b] P values were calculated by the χ^2 test with Yates correction.

($P < 0.05$) as potential predictors of early recurrence. Hierarchical clustering analysis of these genes revealed distinct expression patterns between the recurrence and the recurrence-free group (Fig. 1).

Next, we examined the accuracy of recurrence prediction using these genes based on a WV algorithm with a leave-one-out cross-validation approach. Using all 92 genes for classification, 50 of 60 cases (83.3%) were correctly classified into either the recurrence or the recurrence-free group. These results indicate that these genes provide a valuable assessment of recurrence. To examine whether all of 92 genes are necessary for recurrence prediction, we decreased the number of predictive genes by a leave-one-out cross-validation approach. After ranking the 92 genes according to the P values obtained by permutation testing, we estimated the prediction accuracy with changing the number of genes ranked from 5 to 92 (Fig. 2). The accuracy curve was almost flattened substantially to the highest accuracy (83.3%) between 20 and 92 genes, following which we adopted the use of the top 20 ranked genes as predictive genes in our molecular diagnosis. The list of these 20 genes is shown in Table 3.

3.3. Predictive value of molecular diagnosis

Since the above cross-validation was not complete, it may be necessary to validate the reliability of this molecular prediction method with independent samples. We therefore prepared an independent validation group of 40 patients either in whom intrahepatic recurrence occurred within two years or who remained recurrence-free for at least two years. This molecular diagnosis using 20 predictive genes classified patients into either a 'good signature' group, who were predicted to have no recurrences, or a 'poor signature' group, who were predicted to recur within early postoperative years. As a result, this method correctly predicted the future outcome within two postoperative years in 29 of 40 cases. The prediction accuracy of early intrahepatic recurrence with our molecular diagnosis was 72.5%. The odds ratio for the poor molecular-signature compared with the good signature was 6.8 (95%CI 1.7–27.5, Fisher's $P = 0.010$).

As further analysis to evaluate our novel indicator, we assessed the probability of recurrence curves and overall survival curves. The 2-year recurrence rates in the patients

Table 2
Univariate analysis of clinicopathological factors of patients in the estimation group

Factors		No. of patients	2-Year recurrence rate (%)	*P* value[b]
Age	<65 years	30	63.3	0.243
	≥65 years	30	43.3	
Sex	Male	48	52.1	0.985
	Female	12	58.3	
HBs Ag	Negative	52	50.0	0.282
	Positive	8	75.0	
HCV Ab	Negative	19	47.4	0.478
	Positive	41	56.1	
Child grade	A	42	52.4	0.842
	B	18	55.6	
Liver cirrhosis	Absent	27	55.6	0.466
	Present	33	51.5	
AFP	<100 ng/ml	34	41.2	0.069
	≥100 ng/ml	26	69.2	
Preoperative TAE	Not performed	45	53.3	0.982
	Performed	15	53.3	
Surgical margin	Negative	17	52.9	0.804
	Positive	43	53.5	
Histological grade[a]	Wel	5	40.0	0.777
	Mod	30	53.3	
	Por	25	56.0	
Tumor size	≤2 cm	15	26.7	0.172
	>2 cm	45	62.2	
Tumor multiplicity	Solitary	38	36.8	<0.001
	Multiple	22	81.8	
Microscopic vascular invasion	Absent	40	42.5	0.003
	Present	20	75.0	
Adjuvant therapy	Not performed	55	50.9	0.243
	Performed	5	80.0	

[a] Histological degree of HCC; wel, well differentiated; mod, moderately differentiated; por, poorly differentiated.
[b] *P* values were calculated by the log-rank test.

Table 3
The 20 top-ranked genes predicting early intrahepatic recurrence

Rank[a]	*P* value[b]	Up/down[c]	GenBank ID	Gene Symbol	Gene Name
1	0.00214	Up	NM_001627	*ALCAM*	Activated leukocyte cell adhesion molecule
2	0.00270	Down	AK095284	*FLJ37965*	Hypothetical protein FLJ37965
3	0.00292	Up	NM_004883	*NRG2*	Neuregulin 2
4	0.00304	Up	NM_004360	*CDH1*	Cadherin 1, type 1, E-cadherin (epithelial)
5	0.00312	Up	NM_003617	*RGS5*	Regulator of G-protein signalling 5
6	0.00392	Up	NM_005345	*HSPA1A*	Heat shock 70kDa protein 1A
7	0.00410	Up	NM_004938	*DAPK1*	Death-associated protein kinase 1
8	0.00468	Down	AI581068	*EST*	cDNA clone IMAGE:2139949
9	0.00490	Up	NM_014281	*SIAHBP1*	Fuse-binding protein-interacting repressor
10	0.00560	Down	NM_000876	*M6P/IGF2R*	Insulin-like growth factor 2 receptor
11	0.00650	Down	AW978041	*EST*	EST390150 MAGE resequences
12	0.00654	Down	NM_018206	*VPS35*	Vacuolar protein sorting 35 (yeast)
13	0.00888	Up	NM_004640	*BAT1*	HLA-B associated transcript 1
14	0.00894	Up	NM_002273	*KRT8*	Keratin 8
15	0.00996	Down	NM_005514	*HLA-B*	Major histocompatibility complex, class I, B
16	0.01004	Down	NM_000321	*RB1*	Retinoblastoma 1 (including osteosarcoma)
17	0.01124	Up	NM_021079	*NMT1*	N-myristoyltransferase 1
18	0.01206	Down	NM_002116	*HLA-A*	Major histocompatibility complex, class I, A
19	0.01230	Up	NM_006590	*USP39*	Ubiquitin specific protease 39
20	0.01280	Up	NM_000476	*AK1*	Adenylate kinase 1

[a] Ranking was according to the *P* value.
[b] *P* values were calculated by random permutation test.
[c] Upregulation or downregulation were defined as expression in the recurrence group compared to the recurrence-free group.

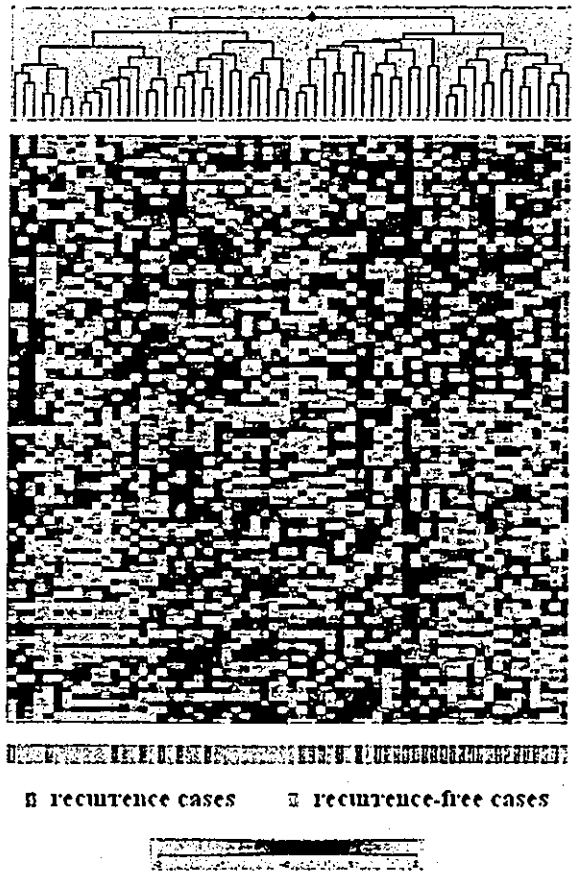

Fig. 1. Hierarchical clustering with 92 selected genes in the estimation group. The rows and columns represent genes and samples, respectively. The bottom scale indicates relative expression level in terms of a standard deviation from the mean.

with the good molecular-signature and those with the poor signature were 29.4 and 73.9%, respectively. The difference of the probability of recurrence between two groups was significant ($P = 0.001$, Fig. 3A). Although a poor survival dose not always reflect early recurrence in the HCC due to several modalities for treatments after recurrence and liver function, survival of the patients with the good molecular-signature was significantly better than that with poor-signature in the present study ($P = 0.036$, Fig. 3B).

3.4. Comparison with conventional prognostic indicators

To compare our molecular prediction method with other conventional prognostic indicators, we performed a multivariate Cox analysis on the validation group (Table 4). As confounding variables, we used three clinicopathological factors: tumor size, tumor multiplicity, and microscopic vascular invasion, because these three factors exhibited correlations with early intrahepatic recurrence that were statistically significant by the χ^2 test or the log-rank test in the estimation group. Molecular-signature was revealed to be an independent factor ($P = 0.007$), and the hazard ratio was 3.82 (95%CI 1.44–10.10). When we added other factors like surgical margin as confounding variables, this result was also similar (data not shown).

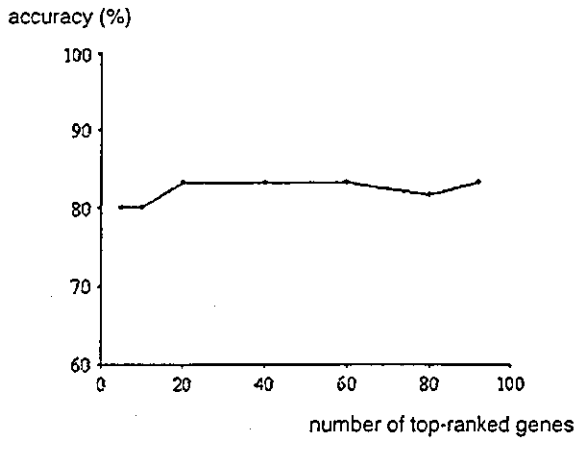

Fig. 2. Accuracy curve of recurrence prediction based on a weighted voting (WV) algorithm with a leave-one-out cross-validation approach in the estimation group. The accuracies in recurrence prediction (y axis) are plotted against the number of used top-ranked genes (x axis).

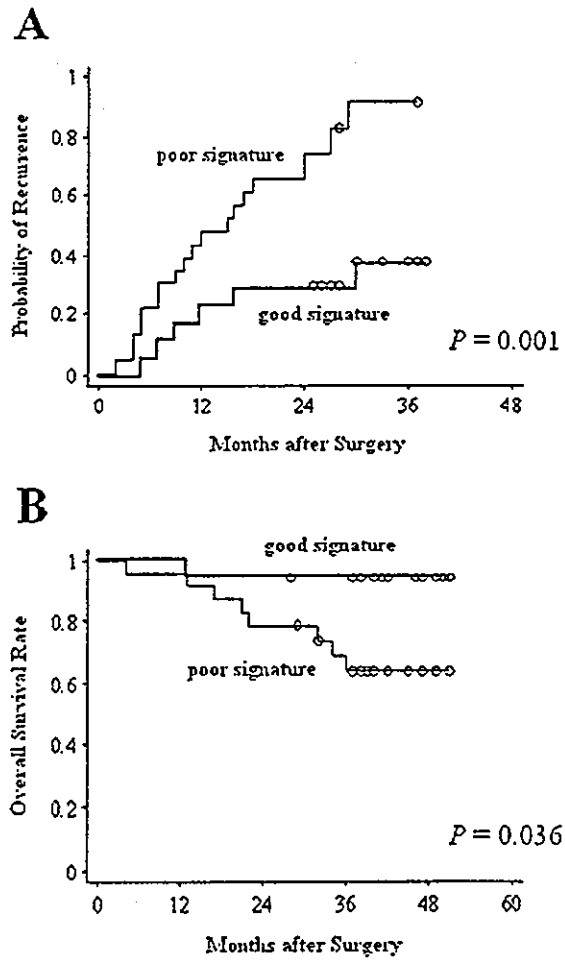

Fig. 3. Probability of recurrence curves (A) and overall survival curves (B) in the validation group. The differences between the good signature group and the poor signature group were analyzed by the log-rank test.

Table 4
Multivariate Cox analysis of clinicopathological factors of patients in the validation group

Factors		2-Year recurrence rate (%)	Hazard ratio	95%CI	*P* value
Molecular-signature	Poor	73.9	3.82	1.44–10.10	0.007
	Good	29.4	1.00	–	–
Tumor size	>2 cm	66.7	1.13	0.35–3.61	0.837
	≤2 cm	30.8	1.00	–	–
Tumor multiplicity	Multiple	78.6	1.97	0.85–4.60	0.116
	Solitary	42.3	1.00	–	–
Microscopic vascular invasion	Present	68.2	1.68	0.62–4.52	0.304
	Absent	38.9	1.00	–	–

4. Discussion

In cancer, the expression of large numbers of genes may be affected. This aberrant transcriptional network is essential for the initiation and maintenance of the malignant phenotype [22]. Although some expression profiling studies in HCC have been performed [23–26], few reports have been able to predict the recurrence or prognosis of HCC patients using a sufficient number of cases. If a molecular method predicting early recurrence could be achieved with high accuracy, it would be possible to make better decisions about the use of adjuvant therapy, such as transcatheter arterial infusions [27], which might improve a patients' prognosis. Unlike other malignancies, however, HCC recurrences derive from residual intrahepatic metastasis (IM) or multicentric carcinogenesis (MC). As MC creates disease foci identical to new tumors occurring in the remnant liver, disease recurrence depended not on the malignant potential of resected HCC, but on the degree of hepatitis or cirrhosis of the remnant liver. Thereby, most late recurrences were considered to be MC [28,29]. In contrast, IM denoted the existence of non-visible intrahepatic metastasis at primary surgery, possibly dependent on the malignant potential of the primary tumor. Although it is difficult to distinguish these patterns of recurrence, IM is likely responsible for the majority of early recurrences, in particular those occurring within the first two postoperative years [28,29]. To predict IM recurrence using gene expression profiles, we divided HCC cases in the estimation group into two groups according to the presence or absence of intrahepatic recurrences at two years after surgery. While a longer follow-up time might be necessary for analysis, our analyzed cases were sufficient for our focus on early recurrence, i.e. IM. TNM staging of HCC, considered to be the most reliable indicator for early recurrence, was estimated using tumor size, tumor multiplicity, vessel invasion, lymph node metastasis, and distant metastasis [21]. In practical cases, however, TNM staging was often insufficient, even when combined with other established indicators [6,7]. Additional factors articulating the biologic characteristics affecting IM should be sought to identify subgroups of patients with similar clinical risk of tumor recurrence.

DNA microarray technology allows for parallel expression analysis of thousands of genes to address complex questions in tumor biology [30]; many trials predicting the prognosis of various human malignancies have been reported using DNA microarrays [31–33]. Although DNA microarrays have contributed to such studies to some degree, molecular-based prediction methods whose real values were estimated with a sufficient number of samples are still rare. DNA microarrays, moreover, have technological limitations, as they can detect only a fraction of the changes in gene expression detectable by RT-PCR [34]. We therefore performed a high throughput quantitative PCR based on ATAC-PCR [9], to analyze the genetic differences in HCC. Using adequate standards, such experiments can be easily controlled. In addition, the assay requires smaller amounts of RNA than DNA microarray analysis. PCR-based analysis of selected genes costs much less than DNA microarrays, likely to require at least several hundreds spotted genes for diagnosis. The aforementioned benefits and the strength of this system for cancer research, established in previous works on not only HCC but also breast or colorectal cancers, makes this technique a powerful method to obtain a better understanding of the molecular characteristics of cancers [11–14].

At first, we identified 92 significant genes by random permutation testing of the estimation group. Hierarchical clustering revealed distinct expression patterns between the recurrence group and the recurrence-free group for these genes. For widespread clinical application of molecular prediction, minimization of the number of predictive genes would be ideal. From these 92 genes, we selected the top 20 ranked genes with the highest prediction accuracy by leave-one-out cross-validation. The 20 predictive genes included various genes demonstrating an association with HCC or other malignancies. *CDH1* encodes the cell adhesion molecule, E-cadherin; loss of E-cadherin function is thought to contribute to progression in cancer by increasing proliferation, invasion, and/or metastasis. Mutations in this gene correlate with many malignancies, and may contribute to early recurrence of HCC [35]. *M6P/IGF2R*, which binds both insulin-like growth factor 2 and mannose 6-phosphate, is a putative hepatocellular tumor suppressor gene.

Evidence of strong correlation to hepatocarcinogenesis was discovered from the loss of heterozygosity [36]; haplo insufficiency is an early event in human hepatocarcinogenesis [37]. *RB1*, which inhibits progression from G1 to S phase in the cell cycle, is a tumor-suppressor gene implicated in a wide variety of cancers. *RB1* expression, assessed by immunohistochemical analysis, is associated with survival in HCC patients [38,39]. The immunoglobulin superfamily member *ALCAM*, activated leucocyte cell adhesion molecule (CD166), binds CD6, to function in interactions among neuronal or immune cells. Correlation with other malignancies has also been reported [40,41]. The *KRT8* protein, a member of a family of structural proteins, may form intermediate filaments. This protein was selected as a differentially expressed gene in other expression profiling studies examining brain tumors and lung cancers [42,43].

In this study, our prediction method using only 20 genes could be validated in an independent dataset. Indeed, the prediction accuracy (72.5%) in the validation group was lower than previously reported studies with DNA microarrays [44,45]. Ye et al. used a compound co-variate predictor algorithm using 153 genes to identify HCC with simultaneous multinodularity. Iizuka et al. used a Fisher linear classifier algorithm containing 12 genes to predict intrahepatic recurrences within one year after surgery. In their validation groups, the predictive accuracy was 85.0% (= 17/20) and 92.6% (= 25/27), respectively. However, it is known that the small sample size can give inflated over-promising results from selection bias or publication bias [46]. Furthermore, recurrence should be analyzed by Kaplan–Meier curves, as recurrence is a time-dependent variable. We have had three cases recur between two and three postoperative years in the poor signature group; thus, the accuracy of our prediction method may be somewhat lower. Comparing the predictive genes between these studies, there were no common genes among three reports. We think the primary reason for this discrepancy was the different algorithms used for prediction. Of course, these differences may also result from distinct end points of studies.

In summary, our methodology illustrates the potential of genomic technologies to advance treatment planning beyond the empiric, towards a more molecularly defined, individualized approach. The combination of our indicator and conventional prognostic indicators such as TNM stage will more accurately predict the patients' outcome, enabling more appropriate therapeutic decisions for HCC patients applying to liver transplantation, a treatment for primary HCC [47–49]. In addition, as our molecular-based prediction method involves only a small number of predictive genes and a simple classification algorithm not requiring statistical software or trained analysts, this approach could be easily applied to a broad clinical setting.

Acknowledgements

We thank Ms Chiyuri Maruyama, Ms Keiko Miyaoka, Ms Mihoko Yoshino and Ms Satoko Maki for expert technical assistance. This work was supported by Grant-in-Aid for the Development of Innovative Technology from the Ministry of Education, Culture, Sports, Science and Technology, Japan.

References

[1] Lai EC, Fan ST, Lo CM, Chu KM, Liu CL, Wong J. Hepatic resection for hepatocellular carcinoma. An audit of 343 patients. Ann Surg 1995;221:291–298.
[2] Poon RT, Fan ST, Lo CM, Ng IO, Liu CL, Lam CM, et al. Improving survival results after resection of hepatocellular carcinoma: a prospective study of 377 patients over 10 years. Ann Surg 2001; 234:63–70.
[3] Ono T, Yamanoi A, El-Assal ON, Kohno H, Nagasue N. Adjuvant chemotherapy after resection of hepatocellular carcinoma causes deterioration of long-term prognosis in cirrhotic patients: meta analysis of three randomized controlled trials. Cancer 2001;91: 2378–2385.
[4] Liver Cancer Study Group of Japan, The general rules for the clinical and pathological study of primary liver cancer, 3rd ed. Tokyo: Kanehara Press; 1992.
[5] Fleming ID, Cooper JS, Henson DE. AJCC cancer staging manual. Philadelphia, PA: Lippincott-Raven; 1997.
[6] Izumi R, Shimizu K, Ii T, Yagi M, Matsui O, Nonomura A, et al. Prognostic factors of hepatocellular carcinoma in patients undergoing hepatic resection. Gastroenterology 1994;106:720–727.
[7] Chiappa A, Zbar AP, Podda M, Audisio RA, Bertani E, Biella F, et al. Prognostic value of the modified TNM (Izumi) classification of hepatocellular carcinoma in 53 cirrhotic patients undergoing resection. Hepatogastroenterology 2001;48:229–234.
[8] Matoba R, Kato K, Kurooka C, Maruyama C, Sakakibara Y, Matsubara K. Correlation between gene functions and developmental expression patterns in the mouse cerebellum. Eur J Neurosci 2002;12: 1357–1371.
[9] Kato K. Adaptor-tagged competitive PCR: a novel method for measuring relative gene expression. Nucleic Acids Res 1997;25: 4694–4696.
[10] Matoba R, Kato K, Saito S, Kurooka C, Maruyama C, Sakakibara Y, et al. Gene expression in mouse cerebellum during its development. Gene 2000;241:125–131.
[11] Kurokawa Y, Matoba R, Takemasa I, Nakamori S, Tsujie M, Nagano H, et al. Molecular features of non-B, non-C hepatocellular carcinoma: a PCR-array gene expression profiling study. J Hepatol 2003;39:1004–1012.
[12] Kurokawa Y, Matoba R, Nakamori S, Takemasa I, Nagano H, Dono K, et al. PCR-array gene expression profiling of hepatocellular carcinoma. J Exp Clin Cancer Res 2004;23:135–141.
[13] Iwao K, Matoba R, Ueno N, Ando A, Miyoshi Y, Matsubara K, et al. Molecular classification of primary breast tumors possessing distinct prognostic properties. Hum Mol Genet 2002;11:199–206.
[14] Muro S, Takemasa I, Oba S, Matoba R, Ueno N, Maruyama C, et al. Identification of expressed genes linked to malignancy of human colorectal carcinoma by parametric clustering of quantitative expression data. Genome Biol 2003;4:R21.
[15] Golub TR, Slonim DK, Tamayo P, Huard C, Gaasenbeek M, Mesirov JP, et al. Molecular classification of cancer: class discovery and class prediction by gene expression monitoring. Science 1999;286: 531–537.

[16] MacDonald TJ, Brown KM, LaFleur B, Peterson K, Lawlor C, Chen Y, et al. Expression profiling of medulloblastoma: PDGFRA and the RAS/MAPK pathway as therapeutic targets for metastatic disease. Nat Genet 2001;29:143–152.
[17] Pomeroy SL, Tamayo P, Gaasenbeek M, Sturla LM, Angelo M, McLaughlin ME, et al. Prediction of central nervous system embryonal tumor outcome based on gene expression. Nature 2002; 415:436–442.
[18] Armstrong SA, Staunton JE, Silverman LB, Pieters R, den Boer ML, Minden MD, et al. MLL translocations specify a distinct gene expression profile that distinguishes a unique leukemia. Nat Genet 2002;30:41–47.
[19] Ramaswamy S, Ross KN, Lander ES, Golub TR. A molecular signature of metastasis in primary solid tumors. Nat Genet 2003;33: 49–54.
[20] van de Vijver MJ, He YD, van't Veer LJ, Dai H, Hart AA, Voskuil DW, et al. A gene-expression signature as a predictor of survival in breast cancer. N Engl J Med 2002;347:1999–2009.
[21] Sobin LH, Wikkekind C, editors. TNM classification of malignant tumours, 5th ed. New York: Wiley; 1997.
[22] Ponder BA. Cancer genetics. Nature 2001;411:336–341.
[23] Okabe H, Satoh S, Kato T, Kitahara O, Yanagawa R, Yamaoka Y, et al. Genome-wide analysis of gene expression in human hepatocellular carcinomas using cDNA microarray: identification of genes involved in viral carcinogenesis and tumor progression. Cancer Res 2001;61:2129–2137.
[24] Shirota Y, Kaneko S, Honda M, Kawai HF, Kobayashi K. Identification of differentially expressed genes in hepatocellular carcinoma with cDNA microarrays. Hepatology 2001;33:832–840.
[25] Xu XR, Huang J, Xu ZG, Qian BZ, Zhu ZD, Yan Q, et al. Insight into hepatocellular carcinogenesis at transcriptome level by comparing gene expression profiles of hepatocellular carcinoma with those of corresponding noncancerous liver. Proc Natl Acad Sci USA 2001;98: 15089–15094.
[26] Chen X, Cheung ST, So S, Fan ST, Barry C, Higgins J, et al. Gene expression patterns in human liver cancers. Mol Biol Cell 2002;13: 1929–1939.
[27] Tanaka K, Shimada H, Togo S, Takahashi T, Endo I, Sekido H, et al. Use of transcatheter arterial infusion of anticancer agents with lipiodol to prevent recurrence of hepatocellular carcinoma after hepatic resection. Hepatogastroenterology 1999;46:1083–1088.
[28] Sakon M, Umeshita K, Nagano H, Eguchi H, Kishimoto S, Miyamoto A, et al. Clinical significance of hepatic resection in hepatocellular carcinoma. Arch Surg 2000;135:1456–1459.
[29] Morimoto O, Nagano H, Sakon M, Fujiwara Y, Yamada T, Nakagawa H, et al. Diagnosis of intrahepatic metastasis and multicentric carcinogenesis by microsatellite loss of heterozygosity in patients with multiple and recurrent hepatocellular carcinomas. J Hepatol 2003;39:215–221.
[30] Shalon D, Smith SJ, Brown PO. A DNA microarray system for analyzing complex DNA samples using two-color fluorescent probe hybridization. Genome Res 1996;6:639–645.
[31] Alizadeh AA, Eisen MB, Davis RE, Ma C, Lossos IS, Rosenwald A, et al. Distinct types of diffuse large B-cell lymphoma identified by gene expression profiling. Nature 2000;403:503–511.
[32] Beer DG, Kardia SL, Huang CC, Giordano TJ, Levin AM, Misek DE, et al. Gene-expression profiles predict survival of patients with lung adenocarcinoma. Nat Med 2002;8:816–824.
[33] Rosenwald A, Wright G, Chan WC, Connors JM, Campo E, Fisher RI, et al. The use of molecular profiling to predict survival after chemotherapy for diffuse large-B-cell lymphoma. N Engl J Med 2002;346:1937–1947.
[34] Holland MJ. Transcript abundance in yeast varies over six orders of magnitude. J Biol Chem 2002;277:14363–14366.
[35] Huang GT, Lee HS, Chen CH, Sheu JC, Chiou LL, Chen DS. Correlation of E-cadherin expression and recurrence of hepatocellular carcinoma. Hepatogastroenterology 1999;46:1923–1927.
[36] De Souza AT, Hankins GR, Washington MK, Orton TC, Jirtle RL. *M6P/IGF2R* gene is mutated in human hepatocellular carcinomas with loss of heterozygosity. Nat Genet 1995;11:447–449.
[37] Oka Y, Waterland RA, Killian JK, Nolan CM, Jang HS, Tohara K, et al. *M6P/IGF2R* tumor suppressor gene mutated in hepatocellular carcinomas in Japan. Hepatology 2002;35:1153–1163.
[38] Naka T, Toyota N, Kaneko T, Kaibara N. Protein expression of p53, p21WAF1, and Rb as prognostic indicators in patients with surgically treated hepatocellular carcinoma. Anticancer Res 1998;18:555–564.
[39] Seki S, Kawakita N, Yanai A, Kitada T, Sakai Y, Nakatani K, et al. Expression of the retinoblastoma gene product in human hepatocellular carcinoma. Hum Pathol 1995;26:366–374.
[40] van Kempen LC, van den Oord JJ, van Muijen GN, Weidle UH, Bloemers HP, Swart GW. Activated leukocyte cell adhesion molecule/CD166, a marker of tumor progression in primary malignant melanoma of the skin. Am J Pathol 2000;156:769–774.
[41] Kristiansen G, Pilarsky C, Wissmann C, Stephan C, Weissbach L, Loy V, et al. ALCAM/CD166 is up-regulated in low-grade prostate cancer and progressively lost in high-grade lesions. Prostate 2003;54:34–43.
[42] Huang H, Colella S, Kurrer M, Yonekawa Y, Kleihues P, Ohgaki H. Gene expression profiling of low-grade diffuse astrocytomas by cDNA arrays. Cancer Res 2000;60:6868–6874.
[43] Wikman H, Kettunen E, Seppanen JK, Karjalainen A, Hollmen J, Anttila S, et al. Identification of differentially expressed genes in pulmonary adenocarcinoma by using cDNA array. Oncogene 2002; 21:5804–5813.
[44] Ye QH, Qin LX, Forgues M, He P, Kim JW, Peng AC, et al. Predicting hepatitis B virus-positive metastatic hepatocellular carcinomas using gene expression profiling and supervised machine learning. Nat Med 2003;9:416–423.
[45] Iizuka N, Oka M, Yamada-Okabe H, Nishida M, Maeda Y, Mori N, et al. Oligonucleotide microarray for prediction of early intrahepatic recurrence of hepatocellular carcinoma after curative resection. Lancet 2003;361:923–929.
[46] Ntzani EE, Ioannidis JP. Predictive ability of DNA microarrays for cancer outcomes and correlates: an empirical assessment. Lancet 2003;362:1439–1444.
[47] Farmer DG, Rosove MH, Shaked A, Busuttil RW. Current treatment modalities for hepatocellular carcinoma. Ann Surg 1994;219: 236–247.
[48] Klintmalm GB. Liver transplantation for hepatocellular carcinoma: a registry report of the impact of tumor characteristics on outcome. Ann Surg 1998;228:479–490.
[49] Yoo HY, Patt CH, Geschwind JF, Thuluvath PJ. The outcome of liver transplantation in patients with hepatocellular carcinoma in the United States between 1988 and 2001: 5-year survival has improved significantly with time. J Clin Oncol 2003;21:4329–4335.

J. Exp. Clin. Cancer Res., 23, 1, 2004

PCR-array Gene Expression Profiling of Hepatocellular Carcinoma

Y. Kurokawa[1], R. Matoba[2], S. Nakamori[1], I. Takemasa[1], H. Nagano[1], K. Dono[1], K. Umeshita[1], M. Sakon[1], M. Monden[1], K. Kato[2]

Dept. of Surgery and Clinical Oncology[1], Graduate School of Medicine, Osaka University, Osaka; Taisho Laboratory of Functional Genomics[2], Nara Institute of Science and Technology, Nara; Japan

Many trials using DNA microarrays have been reported for various human malignancies, but an efficient molecular diagnostic system has yet to be established. Here, we adopted a high throughput quantitative PCR-array system based on adaptor-tagged competitive PCR (ATAC-PCR), as a novel technique for gene expression profiling of hepatocellular carcinoma (HCC). This PCR-array contained 3,072 genes derived from three different cDNA libraries, including 298 additional known genes suspected to be involved in hepatocarcinogenesis. Using this PCR-array with 20 pairs of liver tissues (20 HCC, 20 surrounding nontumor liver), we identified a total of 117 genes differing in expression levels in the two liver tissues. Hierarchical clustering analysis and principal component analysis with these genes revealed distinct gene expression patterns in the HBV-positive group and the HCV-positive groups. Among 117 genes, only 7 (*GPAA1, TMEM9, FACL4, ADFP, MAWBP, PACE4, FOS*) were common to both groups. In conclusion, this PCR-array analysis with an appropriate set of genes is considered useful for gene expression profiling of HCC, and we identified some genes which may play a common key role in hepatocarcinogenesis.

Key Words: Hepatocellular Carcinoma, HCC, PCR-array, ATAC-PCR, DNA microarray, Expression profiling

Hepatocellular carcinoma (HCC), the predominant histological subtype of primary liver cancer, is one of the most common malignancies throughout the world. HCC usually develops with a background of chronic liver inflammation caused by hepatitis virus (HBV, HCV) infection (1). At the molecular level, structural alterations in cancer-related genes such as *p53*, *RB1* and *TGF-beta1* have been reported (2,3), and distinct, but related, genetic pathways may be altered during hepatocarcinogenesis, possibly due to different hepatitis viruses. Until now, although various biological studies of HCC linked to hepatitis viruses have been reported (4,5), it is not known whether the genetic events that occur during the development of HCC differ depending on the hepatitis virus involved.

Gene expression profiling is a powerful new molecular technique for analyzing the expression levels of the entire mRNA population of a specific tissue. DNA microarray technology allows for parallel expression analysis of thousands of genes to address complex questions in tumor biology (6). Many trials using cDNA or oligonucleotide microarrays have been reported in various human malignancies (7-10). Microarrays may, however, detect only a fraction of the changes in gene expression that RT-PCR could (11); thus, different technologies may contribute to better molecular diagnostic systems. Here, we adopted a PCR-array system, a high throughput quantitative PCR based on adaptor-tagged competitive PCR (ATAC-PCR), as a novel technique (12). ATAC-PCR is an advanced version of quantitative competitive PCR, characterized by the addition of 7 adaptors to different cDNAs, and this PCR-based system is much better for detecting subtle changes in gene expression. Since our PCR-array carried thousands of genes which were preferentially expressed in the liver tissues, it augmented sensitivity for detecting bias in cancer. Using this PCR-array, we searched for genes with expression levels in HCC differing from those in nontumor liver tissues, and selected some candidate genes which play a key role in common hepatocarcinogenesis by comparing their expression

in HBV-positive cases and HCV-positive cases.

Materials and Methods

Tissues and Patients. We obtained 20 pairs of liver tissues (20 HCC, 20 nontumor liver) with written informed consent from 20 patients who underwent hepatic resection for HCC at the Osaka University Hospital between 1997 and 2001. Tumor (T) and nontumor (NT) tissue samples were enucleated separately from either the tumorous or nontumorous part of the resected tissues. Serologically, 10 cases were hepatitis B surface antigen-positive and 10 cases were HCV antibody-positive. No cases double-positive for the hepatitis B surface antigen and the HCV antibody were included in this study.

Selection of Genes Expressed in Liver Tissues. To select genes for analysis with the PCR-array system, we constructed three cDNA libraries from a mixture of HCC and nontumor livers, normal livers, and metastatic liver cancers, as described previously (13). For the HCC library, a mixture of total RNAs from 7 HCC and 6 nontumor samples were used, and 2,673 unique sequences were obtained from 9,600 clones. We designed PCR primers for the ATAC-PCR reaction for a total of 2,384 genes from this EST collection. In addition, we prepared 130 primers from the normal liver library and 260 primers from the metastatic liver cancer library. Altogether, we prepared 3,072 primers for ATAC-PCR, including 298 additional known genes from the previous literature.

PCR-array System. A PCR-array is a high-throughput RT-PCR system based on ATAC-PCR, and the experimental procedure was performed as previously described (14). Briefly, 5μg of RNA was converted into cDNA, digested by a restriction enzyme, and then ligated to an adaptor by using the cohesive ends created by the enzyme. After mixing the ligated samples into a single tube, PCR amplification was performed using an adaptor primer and a gene-specific primer. In this study, seven adaptors were used, instead of six, with the two shortest adaptors (MB-1 and -2) used to amplify standard cDNAs of differing amounts. The sequences of the seven adaptors were as follows:

(1S) 5'-GTACATATTGTCGTTAGAACGCG-3'
(1L) 5'-GATCCGCGTTCTAACGACAATATG TAC-3'
(2S) 5'-GTACATATTGTCGTTAGAACGCGACT-3'
(2L) 5'-GATCAGTCGCGTTCTAACGACAATAT GTAC-3'
(3S) 5'-GTACATATTGTCGTTAGAACGCGCAT ACT-3'
(3L) 5'-GATCAGTATGCGCGTTCTAACGA CAATATGTAC-3'
(4S) 5'-GTACATATTGTCGTTAGAACGCGATC CATACT-3'
(4L) 5'-GATCAGTATGGATCGCGTTCTAACGA CAATATGTAC-3'
(5S) 5'-GTACATATTGTCGTTAGAACGCGT CAATCCATACT-3'
(5L) 5'-GATCAGTATGGATTGACGCGTTC TAACGACAATATGTAC-3'
(6S) 5'-GTACATATTGTCGTTAGAACGCG TACTCAATCCATACT-3'
(6L) 5'-GATCAGTATGGATTGAGTACGCGTTC TAACGACAATATGTAC-3'
(7S) 5'-GTACATATTGTCGTTAGAACGCGC TATACTCAATCCATACT-3'
(7L)5'-GATCAGTATGGATTGATAT AGCGCGTTCTAACGACAATATGTAC-3'

The PCR cycling condition was set as follows: an initial denaturing step at 95°C for 10 min and 40 cycles at 94°C for 30 sec, 50°C for 30 sec, and 72°C for 60 sec, followed by an incubation at 72°C for 20 min. We chose a mixture of the 15 HCC and 8 nontumor tissues from HCC patients as the source of the standard, following which we estimated the relative expression levels from the standard expression levels. Each reaction mixture contained ten portions of standard cDNA with the shortest adaptor, two portions of standard cDNA with the second shortest adaptor, and five portions of each sample, where one portion was equivalent to 174 pg total RNA. Amplified products were separated on an ABI 3100 DNA analyzer. A detailed protocol is available at our web site (http://love2.aistnara.ac.jp/laboratory/index_frame.html).

Analysis of PCR-array Data. The calibration curves were made by drawing lines between the origin and the points created by the two standards. For peaks higher than that of MB-1, the line drawn from the origin to the MB-1 point was extrapolated. In cases with no MB-2 peak, a line drawn from the origin to the MB-1 point was used as a calibration curve. In cases where no MB-1 peak existed, or where the MB-2 peak was higher than the MB-1 peak, the missing values were assigned to five samples. Based on these calibration curves, we calculated the relative expression lev-

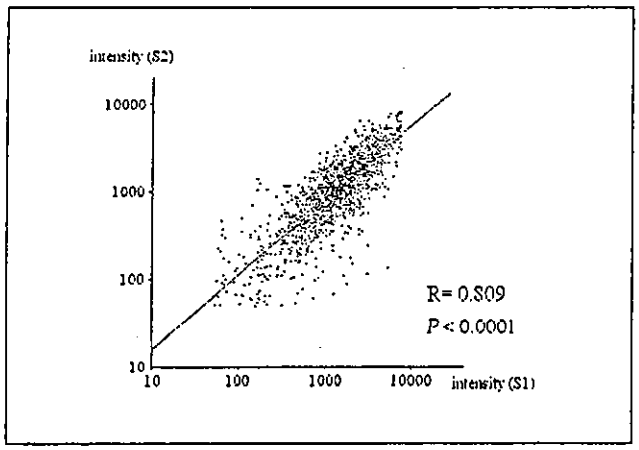

Fig. 1 - Scattergram of the expression data in a PCR-array. The horizontal axis shows the fluorescence intensity of the first ATAC-PCR, and the vertical axis that of the second ATAC-PCR. Their relationship was examined with Pearson's correlation coefficient.

els, following conversion to a logarithmic scale (base 2). Finally, to allow comparison of tumor (T) gene expression values and gene expression values from surrounding nontumor (NT) tissue, T versus NT (T/NT) were estimated for each gene such that $\log_2(T/NT) = \log_2(T) - \log_2(NT)$. Hierarchical cluster analysis, using the Ward method, and principal component analysis (PCA) were performed using GeneMaths 2.0 software.

Results

Before using all samples for this study, we preliminary analyzed the reproducibility of the PCR-array. We repeated ATAC-PCR twice from identical five cDNAs using a 384 PCR-array plate, and obtained a total of 1,920 data points from them. Figure 1 shows a scattergram of the fluorescence intensity scanned after ATAC-PCR, revealing high reproducibility (R=0.809, P<0.0001). This result confirmed the reliability of the PCR-array data using human liver tissues.

Table I - Clinicopathological characteristics between an HBV-positive group and an HCV-positive group

Parameters	HBV-positive group (n=10)	HCV-positive group (n=10)	P value
Age (years)	52 (47-61)	57 (51-67)	0.070
Sex			0.303
Male	6	9	
Female	4	1	
Liver function			0.629
Child A	8	6	
Child B	2	4	
Cirrhosis			>0.999
-	4	4	
+	6	6	
Tumor size (cm)	6.7 (1.1-13.7)	4.9 (1.0-12.5)	0.326
Histological grade of HCC			>0.999
mod	5	4	
por	5	6	
Vessel invasion			>0.999
-	5	4	
+	5	6	
UICC TNM stage			0.601
I	2	4	
II	4	2	
III	2	1	
IV	2	3	

The clinicopathological background of the HBV-positive group (n=10) was compared with that of the HCV-positive group (n=10) by Fisher's exact test, chi square test or Mann-Whitney U test (Table I). None of the factors, that is, age, sex, liver function according to the Child grade, liver cirrhosis, tumor size, histological grade of HCC, vessel invasion, or TNM stage according to UICC classification, showed any significant differences between the two groups.

In order to identify differentially expressed genes in each group, we first calculated the T/NT (tumor versus nontumor) ratios of all genes. When genes with a T/NT ratio of 2 or more in 7 or more of the 10 cases were defined as upregulated genes, 20 and 27 genes were selected as upregulated genes in the HBV-positive group and HCV-positive group, respectively. On the other hand, when genes with a T/NT ratio of 0.5 or less in 7 or more of the 10 cases were defined as downregulated genes, 41 and 36 genes were selected, respectively. These misregulated genes are shown in Table II according to each group, and only 7 genes (*GPAA1, TMEM9, FACL4, ADFP, MAWBP, PACE4, FOS*) were common to both groups.

Next, we performed a hierarchical cluster analysis of samples by the Ward method with these 117 genes. When the clinical samples were sorted on the basis of similarity in the expression of selected genes, they could then be separated according to their infection viruses, *i.e.*, HBV and HCV, with only a few exceptions (Fig. 2). We next applied PCA, a statistical method for reducing the number of data dimensions, in order to more simply present the relationships between the samples. Upon displaying the expression patterns of these 117 genes in three-dimensional space, we observed that HBV-positive cases and HCV-positive cases were located separately, indicating distinct gene expression patterns (Fig. 3). These results indicated that we could select genes representing their characteristic expression profiles in either HBV-positive or HCV-positive cases.

Discussion

With cancer, it is generally accepted that a large number of genes in related pathways are affected at the expression level, and that this aberrant gene transcriptional expression network is essential in the initiation and maintenance of the malignant phenotype. Although the transcriptome analysis of human cancer using cDNA microarrays, oligonucleotide microarrays, as well as serial analysis of gene expression, may provide some clues for understanding oncogenesis, the reliability of these biological technologies is still controversial. With careful planning, we therefore prepared a novel PCR-array system for the following reasons. First, using adequate standards, experiments can be easily controlled. Second, the assay requires far smaller amounts of RNA. Third, the PCR assay of selected genes costs much less than DNA microarrays that are likely to require at least several hundred spotted genes for diagnosis. The results were reproducible, as shown in Figure 1, indicating that the PCR-array is a promising platform for cancer research.

We identified a total of 117 genes which were differentially expressed between tumor (T) tissues and surrounding nontumor (NT) tissues, as they were likely to be involved in the process of hepatocarcinogenesis. These 117 genes included some cancer-related genes which were previously reported to be associated with HCC. As examples, *FOS* has been implicated as a regulator of cell proliferation, differentiation, and transformation, and expression of *FOS* has also been associated with apoptotic cell death. *C-fos*, the human cellular homolog of *v-fos*, a Finkel-Biskis-Jinkins murine osteosarcoma virus oncogene, is well-known to be involved in hepatocarcinogenesis (15,16). *IGFBP3* play a key role in regulating cell proliferation and apoptosis with insulin-like growth factors and their receptors. *IGFBP3* also plays an important inhibitory role in the development and/or growth of HCC (17-19). Likewise, *CD24*, small cell lung carcinoma cluster 4 antigen, differentiates and activates granulocytes and B lymphocytes by glycosyl phosphatidylinositol (GPI) linkage. *CD24* expression appears to be a common event in HCC and may serve as an early, but not prognostic, biomarker for malignant transformation of hepatocytes (20). When compared with the result of previous gene expression profiling study using cDNA microarray (21), six genes (*C9, ALB, CYP2C8, ACADSB, IGFBP3 and ZFP36*) were consistently selected as being differentially expressed between T and NT tissue. As mentioned above, *IGFBP3* has been thought for some time to be intimately involved in the development of HCC. The underexpression of *ALB* mRNA in HCC tissues has been also reported from another expression profiling study (22). Thus, misexpression of these well-known cancer-related genes in our study agreed with the results of most previous reports on HCC cases.

When comparing the differentially expressed genes in an HBV-positive group with an HCV-positive group, only 7 genes (*GPAA1, TMEM9, FACL4, ADFP, MAWBP, PACE4, FOS*) were consistently selected. As

Table II - Differentially expressed genes in HBV-positive cases and HCV-positive cases

HBV-positive cases (n=10)				HCV-positive cases (n=10)			
Num [a]	up/down [b]	*Gene Name*	UniGene ID	Num [a]	up/down [b]	*Gene Name*	UniGene ID
9	up	*KIAA0205*	Hs.3610	10	up	*NICE-3*	Hs.31989
9	up	*ATP6V1E1*	Hs.77805	8	up	*BX1*	Hs.249247
8	up	*GPAA1*	Hs.4742	8	up	*PSMB4*	Hs.89545
8	up	*CGI-149*	Hs.189658	8	up	*KIAA0016*	Hs.75187
8	up	*LAPTM4B*	Hs.296398	8	up	*LEPRE1*	Hs.10114
8	up	*MAZ*	Hs.7647	8	up	*PCNA*	Hs.78996
8	up	*SLC29A1*	Hs.25450	8	up	*S100A10*	Hs.400250
8	up	*KIAA0102*	Hs.77665	8	up	*TMEM9*	Hs.181444
7	up	*SNRPE*	Hs.334612	8	up	*UGDH*	Hs.28309
7	up	*B3GNT6*	Hs.8526	8	up	*HSPA5*	Hs.75410
7	up	*MGC2655*	Hs.400557	7	up	*GPAA1*	Hs.4742
7	up	*HSPCA*	Hs.356531	7	up	*CD24*	Hs.375108
7	up	*FLJ10326*	Hs.262823	7	up	*NME7*	Hs.274479
7	up	*TMEM9*	Hs.181444	7	up	*ALDOC*	Hs.155247
7	up	*FACL4*	Hs.81452	7	up	*SF3B4*	Hs.25797
7	up	*SMT3H2*	Hs.180139	7	up	*MCP*	Hs.83532
7	up	*CCT3*	Hs.1708	7	up	*COL1A2*	Hs.179573
7	up	*TM4SF3*	Hs.84072	7	up	*DDX9*	Hs.74578
7	up	*C1orf37*	Hs.17481	7	up	*DAP13*	Hs.44163
7	up	*COL1A1*	Hs.172928	7	up	*ARL1*	Hs.242894
10	down	*ALDH2*	Hs.195432	7	up	*MRPS23*	Hs.5836
9	down	*ADFP*	Hs.3416	7	up	*FACL4*	Hs.81452
8	down	*CPT2*	Hs.274336	7	up	*KIAA0117*	Hs.322478
8	down	*EPHX2*	Hs.113	7	up	*CYP51*	Hs.226213
8	down	*NDRG2*	Hs.243960	7	up	*TM4SF4*	Hs.11881
8	down	*CYP2J2*	Hs.152096	7	up	*STAM*	Hs.153487
8	down	*PHLDA1*	Hs.82101	7	up	*AIP*	Hs.75305
7	down	*EST*	-	9	down	*ACAA1*	Hs.166160
7	down	*MST1*	Hs.349110	9	down	*ADFP*	Hs.3416
7	down	*FGA*	Hs.351593	8	down	*PACE4*	Hs.170414
7	down	*EHHADH*	Hs.1531	8	down	*FLJ23471*	Hs.156351
7	down	*CP*	Hs.296634	8	down	*HP*	Hs.75990
7	down	*DSCR1*	Hs.184222	8	down	*PEMT*	Hs.15192
7	down	*ADH4*	Hs.1219	8	down	*ETR101*	Hs.737
7	down	*IGFBP3*	Hs.77326	8	down	*PRO1851*	Hs.406267
7	down	*HAO1*	Hs.193640	8	down	*C9*	Hs.1290
7	down	*IDH2*	Hs.5337	8	down	*ZFP36*	Hs.343586
7	down	*APOH*	Hs.1252	8	down	*SLC25A15*	Hs.78457
7	down	*FGL1*	Hs.107	8	down	*GYS2*	Hs.82614
7	down	*FGB*	Hs.7645	7	down	*HF1*	Hs.250651
7	down	*SCP2*	Hs.75760	7	down	*LSM5*	Hs.227280
7	down	*EST*	-	7	down	*CYP3A5P2*	Hs.166079
7	down	*HPX*	Hs.346935	7	down	*SHBG*	Hs.46319
7	down	*PGM1*	Hs.1869	7	down	*FABP1*	Hs.351719
7	down	*MAWBP*	Hs.16341	7	down	*CYP3A4*	Hs.178738
7	down	*PACE4*	Hs.170414	7	down	*ATF5*	Hs.9754
7	down	*A1BG*	Hs.373554	7	down	*MT1G*	Hs.334409
7	down	*HRG*	Hs.1498	7	down	*ALB*	Hs.184411
7	down	*MAT1A*	Hs.323715	7	down	*MAWBP*	Hs.16341
7	down	*CYP2C8*	Hs.174220	7	down	*ANG*	Hs.332764
7	down	*AOX1*	Hs.406238	7	down	*AZGP1*	Hs.71
7	down	*ARG1*	Hs.332405	7	down	*A2M*	Hs.74561
7	down	*ACAA2*	Hs.356176	7	down	*FGG*	Hs.75431
7	down	*ACADSB*	Hs.81934	7	down	*PSMF1*	Hs.75925
7	down	*FLJ39947*	Hs.363456	7	down	*SUCLG2*	Hs.247309
7	down	*ICAM2*	Hs.433303	7	down	*BUCS1*	Hs.98732
7	down	*TDO2*	Hs.183671	7	down	*SSAT2*	Hs.10846
7	down	*EST*	Hs.232042	7	down	*EST*	Hs.378080
7	down	*FOS*	Hs.25647	7	down	*CYP2B6*	Hs.1360
7	down	*PK-120*	Hs.381820	7	down	*RODH*	Hs.11958
7	down	*SLC38A4*	Hs.165655	7	down	*MMP2*	Hs.111301
				7	down	*FOS*	Hs.25647
				7	down	*SERPINA4*	Hs.159628

[a] *number of cases T/NT ratio > 2.0 or < 0.5*

[b] *either upregulated or downregulated in HCC comparing to nontumor liver tissue*

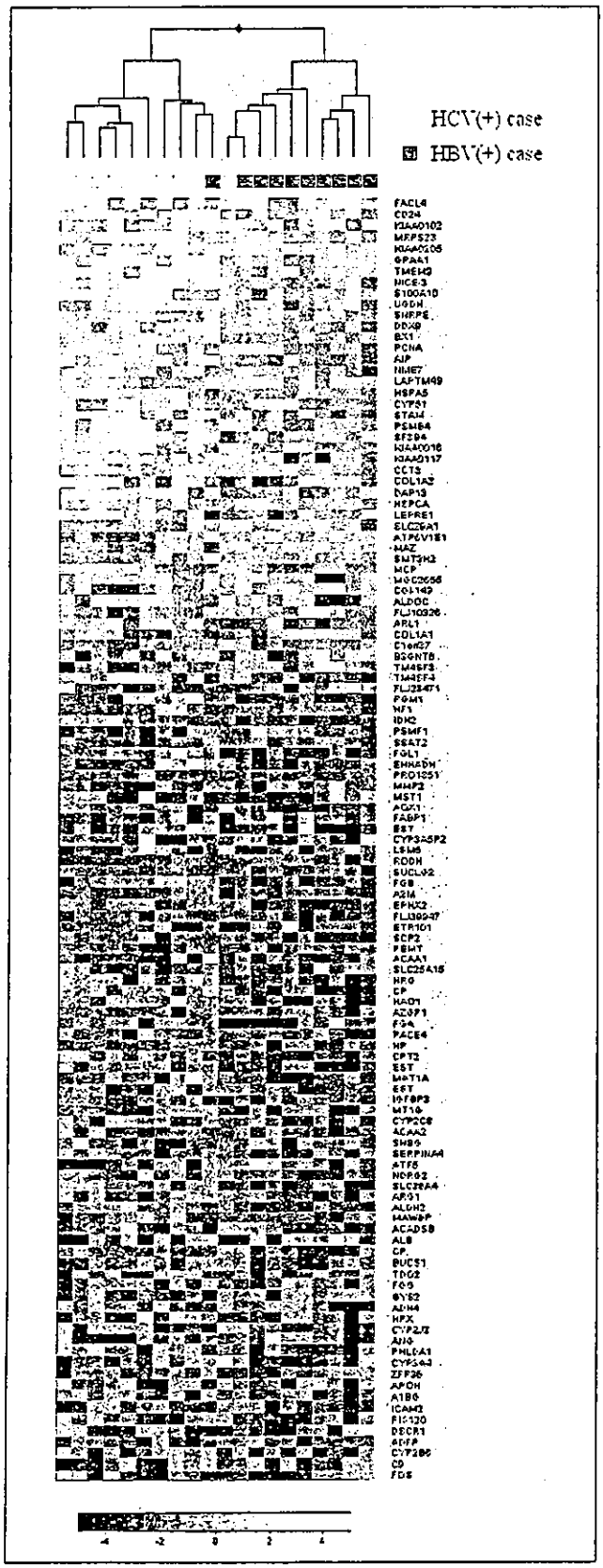

Fig. 2 - Hierarchical clustering of 117 differentially expressed genes by the Ward method. Each row represents a single gene, while each column represents a patient sample. The label of each sample is designated by a crossbar according to the following color categorization: green bars indicate HBV-positive cases, red bars indicate HCV-positive cases. The color scale at the bottom indicates the relative expression levels in terms of the number of standard deviations from the mean.

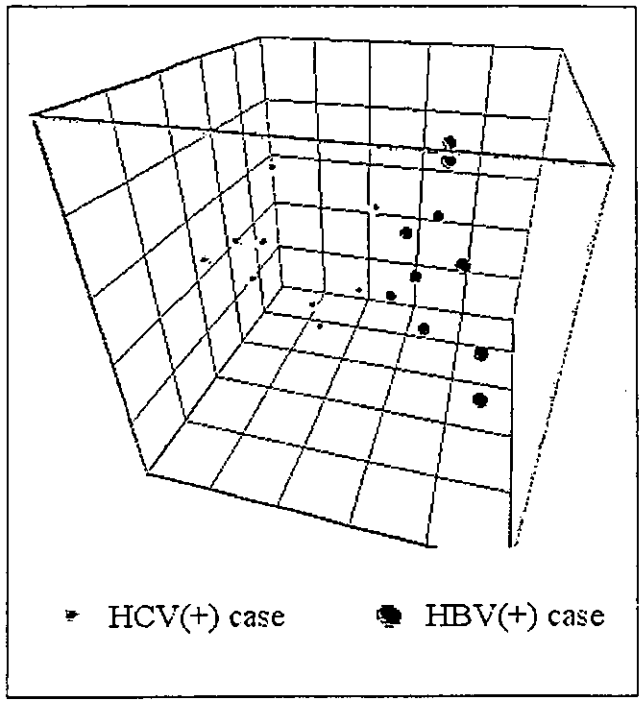

Fig. 3 - Principal component analysis (PCA). The variation is reduced to three-dimensional space, and three components represent 34.5% of total variance. Each sphere represents a single sample: green for HBV-positive case, red for HCV-positive case.

mentioned above, *FOS* has been considered for some time to be closely involved in the development of HCC. On the other hand, most of the differentially expressed genes identified in each group were not identified in the other group. Because the number of samples was small, it may yet be too early to draw conclusions regarding the similarities and differences between the gene expression profiles of HBV-infected HCC and HCV-infected HCC. However, we can at least conclude that these 7 genes are candidate key genes in common hepatocarcinogenesis. Thus, this PCR-array analysis with an appropriate set of genes is

useful for gene expression profiling of HCC. Of course, we need to consider the possibility that the mis-expressions of our selected genes occurred not during the development of HCC but after progression of HCC, and the existence of many differentially expressed genes between T and NT tissue must mean some correlations to hepatocarcinogenesis. Genes that are over-expressed in tumors are therefore potential targets for the rational development of new cancer drugs, and the identification of such targets may improve the efficacy of developing drugs for any cancer.

Acknowledgements: This work was supported in part by Grant-in-Aid for the Development of Innovative Technology from the Ministry of Education, Culture, Sports, Science and Technology of Japan.

References

1. Stuver S.O.: Towards global control of liver cancer? Semin. Cancer Biol. 8:299-306, 1998.
2. Naka T., Toyota N., Kaneko T., Kaibara N.: Protein expression of p53, p21WAF1, and Rb as prognostic indicators in patients with surgically treated hepatocellular carcinoma. Anticancer Res. 18:555-564, 1998.
3. Abou-Shady M., Baer H.U., Friess H., et al.: Transforming growth factor betas and their signaling receptors in human hepatocellular carcinoma. Am. J. Surg. 177:209-215, 1999.
4. Andrisani O.M., Barnabas S.: The transcriptional function of the hepatitis B virus X protein and its role in hepatocarcinogenesis (Review). Int. J. Oncol. 15:373-379, 1999.
5. Bressac B., Kew M., Wands J., Ozturk M.: Selective G to T mutations of p53 gene in hepatocellular carcinoma from southern Africa. Nature 350:429-431, 1991.
6. Shalon D., Smith S.J., Brown P.O.: A DNA microarray system for analyzing complex DNA samples using two-color fluorescent probe hybridization. Genome Res. 6:639-645, 1996.
7. Alizadeh A.A., Eisen M.B., Davis R.E., et al.: Distinct types of diffuse large B-cell lymphoma identified by gene expression profiling. Nature 403:503-511, 2000.
8. van 't Veer L.J., Dai H., van de Vijver M.J., et al.: Gene expression profiling predicts clinical outcome of breast cancer. Nature 415:530-536, 2002.
9. Beer D.G., Kardia S.L., Huang C.C., et al.: Gene-expression profiles predict survival of patients with lung adenocarcinoma. Nat. Med. 8:816-824, 2002.
10. Rosenwald A., Wright G., Chan W.C., et al.: The use of molecular profiling to predict survival after chemotherapy for diffuse large-B-cell lymphoma. N. Engl. J. Med. 346:1937-1947, 2002.
11. Holland M.J.: Transcript abundance in yeast varies over six orders of magnitude. J. Biol. Chem. 277:14363-14366, 2002.
12. Kato K.: Adaptor-tagged competitive PCR: a novel method for measuring relative gene expression. Nucleic Acids Res. 25:4694-4696, 1997.
13. Matoba R., Kato K., Saito S., et al.: Gene expression in mouse cerebellum during its development. Gene 241:125-131, 2000.
14. Matoba R., Kato K., Kurooka C., Maruyama C., Sakakibara Y., Matsubara K.: Correlation between gene functions and developmental expression patterns in the mouse cerebellum. Eur. J. Neurosci. 12:1357-1371, 2002.
15. Arbuthnot P., Kew M., Fitschen W.: C-fos and c-myc oncoprotein expression in human hepatocellular carcinomas. Anticancer Res. 11:921-924, 1991.
16. Yuen M.F., Wu P.C., Lai V.C., Lau J.Y., Lai C.L.: Expression of c-Myc, c-Fos, and c-jun in hepatocellular carcinoma. Cancer 91:106-112, 2001.
17. Gong Y., Cui L., Minuk G.Y.: The expression of insulin-like growth factor binding proteins in human hepatocellular carcinoma. Mol. Cell Biochem. 207:101-104, 2000.
18. Huynh H., Chow P.K., Ooi L.L., Soo K.C.: A possible role for insulin-like growth factor-binding protein-3 autocrine/paracrine loops in controlling hepatocellular carcinoma cell proliferation. Cell Growth Differ. 13:115-122, 2002.
19. Hanafusa T., Yumoto Y., Nouso K., et al.: Reduced expression of insulin-like growth factor binding protein-3 and its promoter hypermethylation in human hepatocellular carcinoma. Cancer Lett. 176:149-158, 2002.
20. Huang L.R., Hsu H.C.: Cloning and expression of CD24 gene in human hepatocellular carcinoma: a potential early tumor marker gene correlates with p53 mutation and tumor differentiation. Cancer Res. 55:4717-4721, 1995.
21. Okabe H., Satoh S., Kato T., et al.: Genome-wide analysis of gene expression in human hepatocellular carcinomas using cDNA microarray: identification of genes involved in viral carcinogenesis and tumor progression. Cancer Res. 61:2129-2137, 2001.
22. Kinoshita M., Miyata M.: Underexpression of mRNA in human hepatocellular carcinoma focusing on eight loci. Hepatology 36:433-438, 2002.

A selected article from JSGC

Kikuya Kato, MD, Ph.D.
Taisho Laboratory of Functional Genomics,
Nara Institute of Science and Technology,
8916-5, Takayama-cho, Ikoma-city,
Nara 630-0101, Japan.
Tel.: +81-743-72-5580; Fax: +81-743-72-5589
E-mail: kkato@bs.aist-nara.ac.jp

Partial Contribution of Tumor Necrosis Factor-Related Apoptosis-Inducing Ligand (TRAIL)/TRAIL Receptor Pathway to Antitumor Effects of Interferon-α/5-Fluorouracil against Hepatocellular Carcinoma

Tameyoshi Yamamoto,[1] Hiroaki Nagano,[1] Masato Sakon,[1] Hisashi Wada,[1] Hidetoshi Eguchi,[1] Motoi Kondo,[1] Bazarragchaa Damdinsuren,[1] Hideo Ota,[1] Masato Nakamura,[1] Hiroshi Wada,[1] Shigeru Marubashi,[1] Atsushi Miyamoto,[1] Keizo Dono,[1] Koji Umeshita,[1] Shoji Nakamori,[1] Hideo Yagita,[2] and Morito Monden[1]

[1]Department of Surgery and Clinical Oncology, Graduate School of Medicine, Osaka, University, Osaka, Japan; [2]Department of Immunology, Juntendo University School of Medicine, Tokyo, Japan

ABSTRACT

Purpose: Our purpose was to explore the contribution of tumor necrosis factor-related apoptosis-inducing ligand (TRAIL)/TRAIL receptor pathway to antitumor effects of IFNα and 5-fluorouracil (5-FU) combination therapy for hepatocellular carcinoma (HCC).

Experimental Design: Susceptibility of HCC cell lines to TRAIL and/or 5-FU was examined by 3-(4,5-dimethylthiazol-2-yl)-2,5-diphenyltetrazolium bromide assay. The effects of 5-FU, IFNα, or both on the expression of TRAIL receptors (R1, R2, R3, and R4) on HCC cells or TRAIL in peripheral blood mononuclear cells (PBMC) were examined by flow cytometry. IFNα-induced cytotoxic effects of PBMC on HCC cell lines were examined by ^{51}Cr release assay. TRAIL expression in peripheral blood mononuclear cells and liver tissue from patients was examined by real-time reverse transcription-PCR or immunohistochemistry.

Results: HLE and HepG2 were sensitive to TRAIL, but HuH7, PLC/PRF/5, and HLF were resistant. 5-FU had synergistic effect on TRAIL in HLF and additive effect in four other HCC cell lines. TRAIL receptors on HCC cells were up-regulated by 5-FU, and IFNα induced TRAIL on $CD4^+$ T cells, $CD14^+$ monocytes, and $CD56^+$ NK cells. Treatment of effector cells by IFNα and target HCC cells by 5-FU enhanced the cytotoxicity of $CD14^+$ monocytes and $CD56^+$ NK cells against HCC cells via a TRAIL-mediated pathway. TRAIL mRNA overexpression was noted in PBMC of HCC patients who clinically responded to IFNα/5-FU combination therapy, and $TRAIL^+$ mononuclear cells were found in cancer tissue of a responder.

Conclusion: Our results suggest that modulation of TRAIL/TRAIL receptor-mediated cytotoxic pathway might partially contribute to the anti-HCC effect of IFNα and 5-FU combination therapy.

INTRODUCTION

Hepatocellular carcinoma (HCC) is one of the most common solid tumors worldwide (1). The prognosis of HCC is still poor despite newly developed therapeutic modalities such as radiofrequency ablation and microwave coagulation therapy (2, 3). HCCs with macroscopic tumor thrombi in the major branches of the portal vein (Vp3–4) are extremely aggressive (4). Most HCC patients with Vp3–4 tumors develop recurrences, and half of them die within 1 year after surgery even if curative resection is done (5). The prognosis of unresectable cases with Vp3–4 is much worse, and most patients die within several months (6). Therefore, the development of new antitumor therapy for HCC patients is urgent and mandatory.

In general, HCCs are resistant to anticancer drugs (7). However, recent studies including those from our group showed an excellent clinical response to the combination therapy of IFNα and 5-fluorouracil (5-FU) in HCC patients complicated with Vp3–4 (8). Although the exact mechanism of action of this combination therapy has not yet been established, it has been reported that IFNα enhances the expression of thymidine phosphorylase in colon carcinoma cells, which converts 5-FU to an active metabolite and enhances the DNA damage by 5-FU (9, 10). We also showed previously that IFNα and 5-FU synergistically reduced tumor cell proliferation through cell cycle arrest (11). Although IFNα also exerts immunomodulatory effects by stimulating T cells, NK cells, and monocytes (12, 13), the involvement of its immunomodulatory properties in the IFNα/5-FU combination therapy remains to be determined.

Recently, IFNα was reported to up-regulate tumor necrosis factor-related apoptosis-inducing ligand (TRAIL) in T cells, NK cells, and monocytes (14–16). TRAIL is a newly identified member of the tumor necrosis factor superfamily, which induces apoptosis of transformed cells but not normal cells (17, 18). TRAIL binds to four distinct membrane-bound TRAIL receptors (TRAIL-R1, R2, R3, and R4) and a soluble receptor, osteoprotegerin. TRAIL-R1 and R2 act as death-inducing recep-

Received 4/26/04; revised 8/22/04; accepted 8/31/04.
Grant support: by a Grant-in-Aid for Cancer Research from the Ministry of Health and Welfare of Japan.
The costs of publication of this article were defrayed in part by the payment of page charges. This article must therefore be hereby marked *advertisement* in accordance with 18 U.S.C. Section 1734 solely to indicate this fact.
Requests for reprints: Hiroaki Nagano, Department of Surgery and Clinical Oncology, Graduate School of Medicine, Osaka University, 2-2 Yamadaoka, Suita City, Osaka 565-0871, Japan. Phone: 81-6-6879-3251; Fax: 81-6-6879-3259; E-mail: hnagano@surg2.med.osaka-u.ac.jp.

tors, whereas TRAIL-R3, -R4, and osteoprotegerin may act as decoy receptors (19–24). An important role for TRAIL in tumor immunotherapy has been suggested in murine models (25). Therefore, the TRAIL/TRAIL receptor system may be involved in the antitumor effect of the IFNα and 5-FU combination therapy.

In the present study, we investigated the effects of IFNα combined with 5-FU on the expression and function of TRAIL and TRAIL receptors in human peripheral blood mononuclear cells (PBMC) and HCC cell lines. We also investigated clinical relevance of the *in vitro* findings by using clinical samples from HCC patients who received the combination therapy. The results suggest the partial contribution of TRAIL/TRAIL receptor-mediated cytotoxic pathway to the tumoricidal effects of IFNα and 5-FU combination therapy on HCC.

MATERIALS AND METHODS

Cells. Human HCC cell lines (HuH7, PLC/PRF/5, HLE, HLF, and HepG2) were obtained from Japan Cancer Research Resources Bank (Osaka, Japan) and maintained in DMEM supplemented with 10% fetal bovine serum and 1% penicillin at 37°C in a humidified incubator under 5% CO_2 in air. PBMC were obtained from healthy subjects and prepared by Ficoll-Hypaque centrifugation. $CD4^+$ T cells, $CD8^+$ T cells, $CD14^+$ monocytes, $CD56^+$ NK cells, $CD19^+$ B cells, $CD4^-CD8^-$ cells, $CD4^-CD8^-CD14^-$ cells, $CD4^-CD8^-CD56^-$ cells, and $CD4^-CD8^-CD14^-CD56^-$ cells were isolated from PBMC by using anti-CD4, anti-CD8, anti-CD14, anti-CD56, and anti-CD19 immunomagnetic beads and Magnetic Cell Sorting (Miltenvi Biotec, Bergisch Gladbach, Germany). The purity of each subset was >90% as determined by flow cytometry. These cells were cultured in RPMI 1640 supplemented with 10% fetal bovine serum and 1% penicillin.

Reagents. Purified human IFNα was obtained from Otsuka Pharmaceutical Co. (Tokushima, Japan), and 5-FU was a kind gift from Kyowa Hakko Co. (Tokyo, Japan). Antihuman TRAIL monoclonal antibody (mAb; RIK-2) was prepared as described previously (26). mAbs against TRAIL receptors were obtained from eBioscience (San Diego, CA).

3-(4,5-Dimethylthiazol-2-yl)-2,5-diphenyltetrazolium bromide Assay. The sensitivity of each HCC cell line to recombinant TRAIL and the effect of 5-FU on TRAIL-induced death were examined by 3-(4,5-dimethylthiazol-2-yl)-2,5-diphenyltetrazolium bromide assay. HCC cells (3×10^3 in 100 μL medium) were seeded in 96-well microplates. After 24 hours, 100-μL medium containing soluble human TRAIL (Alexis Corp., Lausen, Switzerland) and/or 5-FU (Kyowa Corp., Tokyo) were added, and the plates were incubated for 48 hours. Cell viability was assessed by using 3-(4,5-dimethylthiazol-2-yl)-2,5-diphenyltetrazolium bromide solution (Sigma Chemical, St. Louis, MO) according to the instructions provided by the manufacturer, and each well was measured spectrophotometrically on a dual beam microtiter plate reader at 550 nm with a 650-nm reference.

Flow Cytometry. Cells (1×10^6) were incubated with 1 μg of biotinylated mAb against TRAIL and TRAIL receptors or control IgG for 30 minutes at 4°C, followed by phycoerythrin-labeled avidin (BD PharMingen, San Diego, CA). After washing with PBS, the cells were analyzed on a fluorescence-activated cell sorter (FACScan, BD PharMingen), and data were processed with Cell Quest software (BD PharMingen). For detection of TRAIL on $CD4^+$ T cells, $CD8^+$ T cells, $CD14^+$ monocytes, and $CD56^+$ NK cells, PBMCs were double-stained with biotinylated antihuman TRAIL mAb followed by phycoerythrin-labeled avidin and FITC-labeled antihuman CD4, CD8, CD14, or CD56 mAb (BD PharMingen). The mean fluorescence intensity was measured in the experiment of alteration of TRAIL receptors.

^{51}Cr Release Assay. Target HCC cells (1×10^6) were labeled with 40 μCi $Na^{51}CrO_4$ for 45 minutes at 37°C. ^{51}Cr-labeled target cells (1×10^4) and effector cells ($CD4^+$ T cells, $CD8^+$ T cells, $CD4^-CD8^-$ cells, $CD4^-CD8^-CD14^-$ cells, $CD4^-CD8^-CD56^-$ cells, or $CD4^-CD8^-CD14^-CD56^-$ cells) were mixed in U-bottomed wells of a 96-well microplate at the indicated E:T ratios. After 8 hours of incubation, cell-free supernatants were collected and counted on a gamma counter. The following formula was used to calculated the percentage of specific cytotoxicity: [(experimental release − spontaneous release)/(total release − spontaneous release)] × 100. Total or spontaneous release was determined in the presence of 1% NP40 or medium alone, respectively. In some experiments, anti-TRAIL mAb was added at a final concentration of 10 μg/mL.

Quantitative RT-PCR for TRAIL mRNA. Between April 1998 and December 2001, 23 patients with unresectable HCC associated with multiple intrahepatic tumors and Vp3–4 received IFNα/5-FU combination therapy at the Department of Surgery, Osaka University Hospital. The treatment regimen consisted of subcutaneous injection of IFNα (5×10^6 units) on days 1, 3, and 5 of every week for 4 weeks and continuous infusion of 5-FU (450–500 mg/day) for 2 weeks through a catheter introduced into the proper hepatic artery (8). Peripheral blood samples were obtained from 12 patients who received this combination therapy. The study protocol was approved by the Human Ethics Review Committee of Osaka University School of Medicine, and a signed consent form was obtained from each patient before participation in the study. PBMC were prepared by Ficoll-Hypaque centrifugation. We extracted total cellular RNA from PBMC using TRIzol reagent (Molecular Research Center, Cincinnati, OH), using the instructions provided by the manufacturer. Isolated RNA was quantitated and assessed for purity by UV spectrophotometry. cDNA was synthesized with avian myeloblastosis virus reverse transcriptase according to the protocol provided by the supplier (Promega, Madison, WI). One μg of RNA was incubated at 70°C for 5 minutes and then placed on ice before the addition of reverse transcription (RT) reaction reagents with oligodeoxythymidylic acid primer. The RT reaction was done at 42°C for 90 minutes, followed by heating at 95°C for 5 minutes. The LightCycler PCR and detection system (Roche Diagnostics, Mannheim, Germany) was used for amplification and quantification. For detection of glyceraldehyde-3-phosphate dehydrogenase (GAPDH) and TRAIL PCR products, LightCycler DNA Master SYBR Green I (Boehringer Mannheim) was used. We did real-time PCR reactions in a sample mixture containing 0.2 μmol/L of each primer, 1× LC-DNA Master SYBR Green I, 4 mmol/L $MgCl_2$, and 2 μL of cDNA as a template using the following primers: human GAPDH

(forward, 5′-CAACTACATGGTTTACATGTTC-3′; reverse, 5′-GCCAGTGGACTCCACGAC-3′); and human TRAIL (forward, 5′-CAACTCCGTCAGCTCGTTAGAAAG-3′; reverse: 5′-TTAGACCAACAACTATTTCTAGCACT-3′), yielding products of 182 and 443 bp, respectively. GAPDH PCR cycle condition was set up as follows: one cycle of 95°C for 10 minutes followed by 40 cycles of 95°C for 15 seconds, 55°C for 10 seconds, and 72°C for 20 seconds. TRAIL PCR cycle condition was set up as follows: one cycle of 95°C for 10 minutes followed by 35 cycles of 95°C for 15 seconds, 55°C for 10 seconds, and 72°C for 25 seconds. Fluorescence was acquired at the end of every 72°C extension phase. We did quantitative analysis of data using the LightCycler analysis software (Roche Diagnostics). The standard curves for GAPDH and TRAIL were constructed by using 10-fold serial dilutions of cDNA prepared from IFNα-stimulated PBMC from a healthy subject. Expression of TRAIL mRNA was reported relative to GAPDH. In the experiment investigating TRAIL mRNA expression in $CD14^+$ monocytes, $CD56^+$ NK cells, and $CD19^+$ B cells, we did quantitative RT-PCR for TRAIL using the same method.

Immunohistologic Staining for TRAIL-R1 and R2. Paraffin-embedded sections (5-μm thick) of liver cancer tissues from three patients with HCC who responded to IFNα/5-FU combination therapy (responders) and one patient who did not respond to the same therapy (nonresponder) were deparaffinized in xylene and rehydrated before analysis. Endogenous peroxidase was quenched with 0.5% hydrogen peroxide. After washing with PBS, slides were blocked with 1% normal goat serum or normal rabbit serum and then incubated overnight at 4°C at 1:40 dilution in PBS of rabbit anti-DR4 (TRAIL-R1) polyclonal antibody (Santa Cruz Biotechnology, Santa Cruz, CA), goat anti-DR5 (TRAIL-R2) polyclonal antibody (Santa Cruz Biotechnology), or normal rabbit IgG (as a control). En-Vision ABC detection kit (Dako, Tokyo, Japan) containing horseradish peroxidase was used to detect antibody binding. Diaminobenzidine was used as the substrate. Slides were counterstained with hematoxylin.

Immunohistologic Staining for TRAIL. Paraffin-embedded sections (5-μm thick) of liver cancer tissues from three responders and one nonresponder and normal liver tissues from a patient with focal nodular hyperplasia were deparaffinized in xylene and rehydrated before analysis. After washing with PBS, slides were blocked with 2-nitro-5-thiobenzoate blocking buffer (NEN Life Science Products, Boston, MA) and then incubated overnight at 4°C with goat antihuman TRAIL antibody K-18 (Santa Cruz Biotechnology) diluted in 2-nitro-5-thiobenzoate blocking buffer at a concentration of 5 μg/mL. After washing with PBS, slides were incubated with biotinylated donkey antigoat IgG antibody (Chemicon, Temecula, CA) for 30 minutes. Alexa 568-labeled streptavidin (Molecular Probes, Inc., Eugene, OR) was used to detect antibody binding. Slides were then covered with VECTASHIELD (Vector Laboratories, Burlingame, CA) and examined under a confocal laser scanning microscope (model LSM 510, Carl Zeiss, Oberkochen, Germany). A single beam from a helium/neon laser (543 nm) was used for excitation. Emission (603 nm) was detected through a long pass filter (>560 nm) and displayed in red. For control staining, the immunizing peptide K-18p (Santa Cruz Biotechnology) was included at 4 μg/mL in the primary antibody incubation. Placental tissue was used as a positive control (27). The number of TRAIL-positive cells was counted in more than six 360 magnification fields of confocal laser scanning microscope.

Statistical Analysis. Data are represented as mean ± SD or SEM. Differences between groups were examined for significant differences by unpaired *t* test. In Fig. 1*A*, differences in the mean percentages of cell viability in the presence of TRAIL alone or TRAIL plus 5-FU were compared by the Dunnett post hoc procedure. The level of statistical significance was set at $P < 0.05$.

Evaluation of TRAIL/5-FU Cooperative Effects. Calculation of the synergistic cytotoxicity of soluble human TRAIL and 5-FU was determined by isobolographic analysis of Berenbaum (28).

RESULTS

Sensitivity of HCC Cell Lines to TRAIL. We did 3-(4,5-dimethylthiazol-2-yl)-2,5-diphenyltetrazolium bromide assay using soluble human TRAIL to examine the sensitivity of HCC cell lines to TRAIL-mediated cytotoxicity. HuH7, PLC/PRF/5, HLE, HLF, and HepG2 cells were incubated with or without various concentrations of soluble TRAIL and/or 5-FU for 48 hours. Sensitivity to TRAIL or 5-FU was different among five HCC cell lines (Fig. 1*A*). HLE and HepG2 cells were sensitive to soluble human TRAIL, but HuH7, PLC/PRF/5, and HLF cells were rather resistant. On the other hand, 5-FU alone exhibited dose-dependent cytotoxicity against HuH7, PLC/PRF/5, HLF, and HepG2 cells, whereas HLE cells were relatively resistant. The percentage of cell viabilities was significantly decreased by the combined treatment of cells with TRAIL and 5-FU at various doses of these agents as compared with TRAIL alone. Isobologram analysis showed that the combination of TRAIL and 5-FU exhibited a synergistic effect in HLF cells and an additive effect in HuH7, PLC/PRF/5, HLE, and HepG2 cells (Fig. 1*B*).

Expression of TRAIL Receptors on HCC Cell Lines. Using flow cytometry, we investigated whether the difference in HCC cell sensitivity to TRAIL correlated with the expression levels of TRAIL-R1, R2, R3, and R4 on the surface of HCC cell lines (Fig. 2*A*). Low expression levels of TRAIL-R1 were noted on the surface of PLC/PRF/5, HLE, and HLF cells. In addition, TRAIL-R2 was expressed on all HCC cell lines, the expression level was higher on TRAIL-sensitive HCC cells (HLE and HepG2 cells) than on TRAIL-resistant HCC cells (HuH7, PLC/PRF/5, and HLF cells). TRAIL-R3 and R4 were not detectable on the surface of any HCC cell line, regardless of their TRAIL sensitivity status. These results indicate that the basal expression of TRAIL-R2 correlates with the sensitivity to TRAIL.

Effect of 5-FU and/or IFNα on TRAIL Receptor Expression on HCC Cell Lines. To examine the effect of 5-FU and/or IFNα on TRAIL receptor expression on HCC cell lines, the cells were preincubated with or without 5-FU (0.5 μg/mL) and/or IFNα (500 units/mL) for 48 hours followed by determination of expression of TRAIL receptors by flow cytometry. As shown in Fig. 2*B*, preincubation with 5-FU for 48 hours increased the expression of TRAIL-R1, R2, R3, and R4 on HepG2 cells. In contrast, IFNα did not alter the expression of any

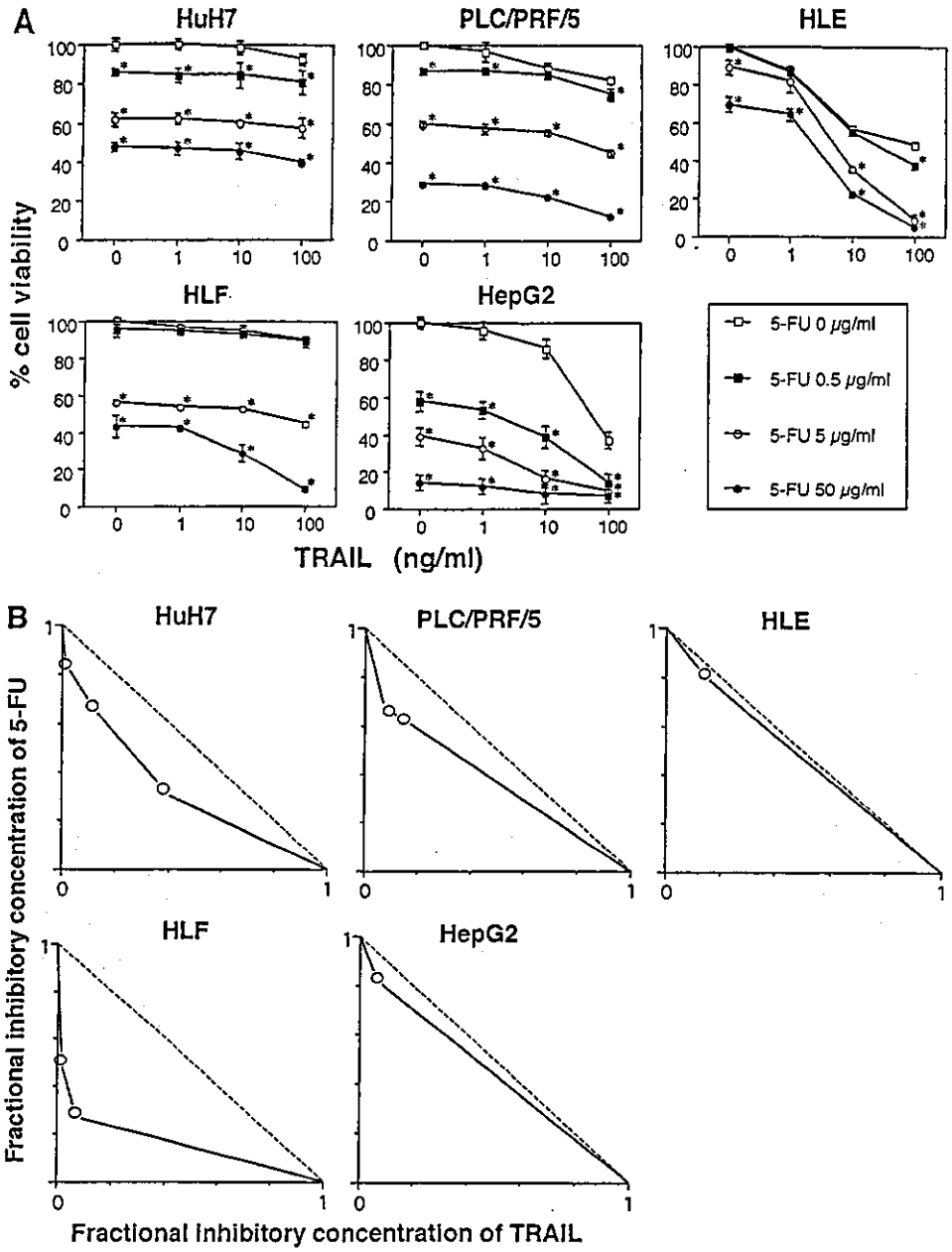

Fig. 1 Effects of 5-FU on TRAIL-induced cytotoxicity in HCC cell lines. *A*, HuH7, PLC/PRF/5, HLE, HLF, and HepG2 cells were treated simultaneously with the indicated concentrations of soluble human TRAIL and 5-FU for 48 hours. 3-(4,5-Dimethylthiazol-2-yl)-2,5-diphenyltetrazolium bromide assay was done to evaluate cell viability. Data are represented as mean ± SD of triplicate samples. Similar results were obtained in three independent experiments. Differences in the percentage of cell viability between TRAIL alone and TRAIL plus 5-FU were determined by the Dunnett post hoc procedure. *, $P < 0.05$. *B*, synergy was estimated by isobolographic analysis.

TRAIL receptor. The effect of combination of 5-FU and IFNα was nearly equal to that of 5-FU alone. As summarized in Fig. 2*C*, the effects of 5-FU and/or IFNα on the expression of TRAIL receptors on other HCC cell lines were similar to the HepG2 case, except for HLE cells, which showed no changes in response to either 5-FU or IFNα. These results indicate that 5-FU, but not IFNα, can significantly increase the expression of TRAIL-R1 and R2 on some HCC cell lines.

Effect of 5-FU and/or IFNα on TRAIL Expression on PBMC. We next examined the effects of 5-FU and/or IFNα on TRAIL expression on PBMC subpopulations (Fig. 3*A*). TRAIL expression was not detected on freshly prepared PBMC by flow cytometry. Incubation with IFNα (500 units/mL) for 24 hours markedly induced TRAIL expression on $CD14^+$ monocytes and $CD56^+$ NK cells. $CD4^+$ T cells, but not $CD8^+$ T cells, also expressed TRAIL at a low level after IFNα stimulation. On the other hand, 5-FU (0.5 μg/mL) did not induce TRAIL expression alone or altered the effect of IFNα on TRAIL expression. IFNα treatment resulted in overexpression of TRAIL mRNA in $CD14^+$ monocytes and $CD56^+$ NK cells. In contrast, no such increase was noted in $CD19^+$ B cells (Fig. 3*B*).

Involvement of TRAIL in IFNα-Stimulated PBMC Cytotoxicity against 5-FU-Treated HCC Cells. We did the ^{51}Cr release assay to investigate the involvement of TRAIL in

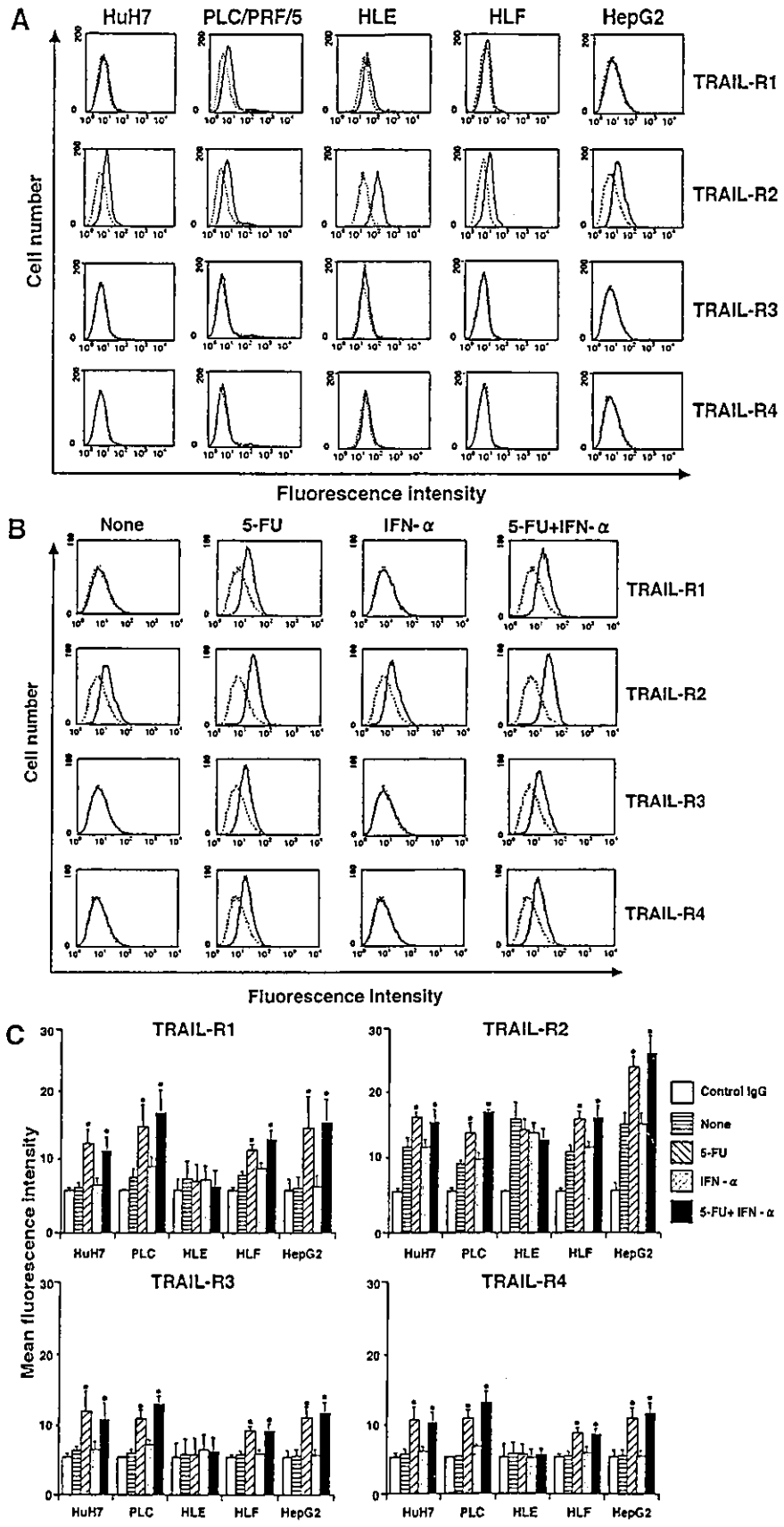

Fig. 2 *A*, Expression of TRAIL receptors on the surface of HCC cell lines. *Dotted lines*, staining with biotinylated control IgG; *solid lines*, staining with biotinylated mAb against the indicated TRAIL receptors. *B* and *C*, effects of 5-FU and/or IFNα on TRAIL receptor expression on HCC cell lines. HepG2 cells (*B*) and the indicated HCC cells (*C*) were treated with 5-FU (0.5 μg/mL) and/or IFNα (500 units/mL) for 48 hours. *B*, *dotted lines*, staining with biotinylated control IgG; *solid lines*, staining with biotinylated mAb against the indicated TRAIL receptors. Similar results were obtained in three independent experiments. *C*, *open bars*, the mean fluorescence intensity of staining with biotinylated control IgG; *other bars*, the mean fluorescence intensity of staining with biotinylated mAbs against the indicated TRAIL receptors. Data are mean ± SD of three independent experiments. *, $P < 0.05$ compared with untreated cells.

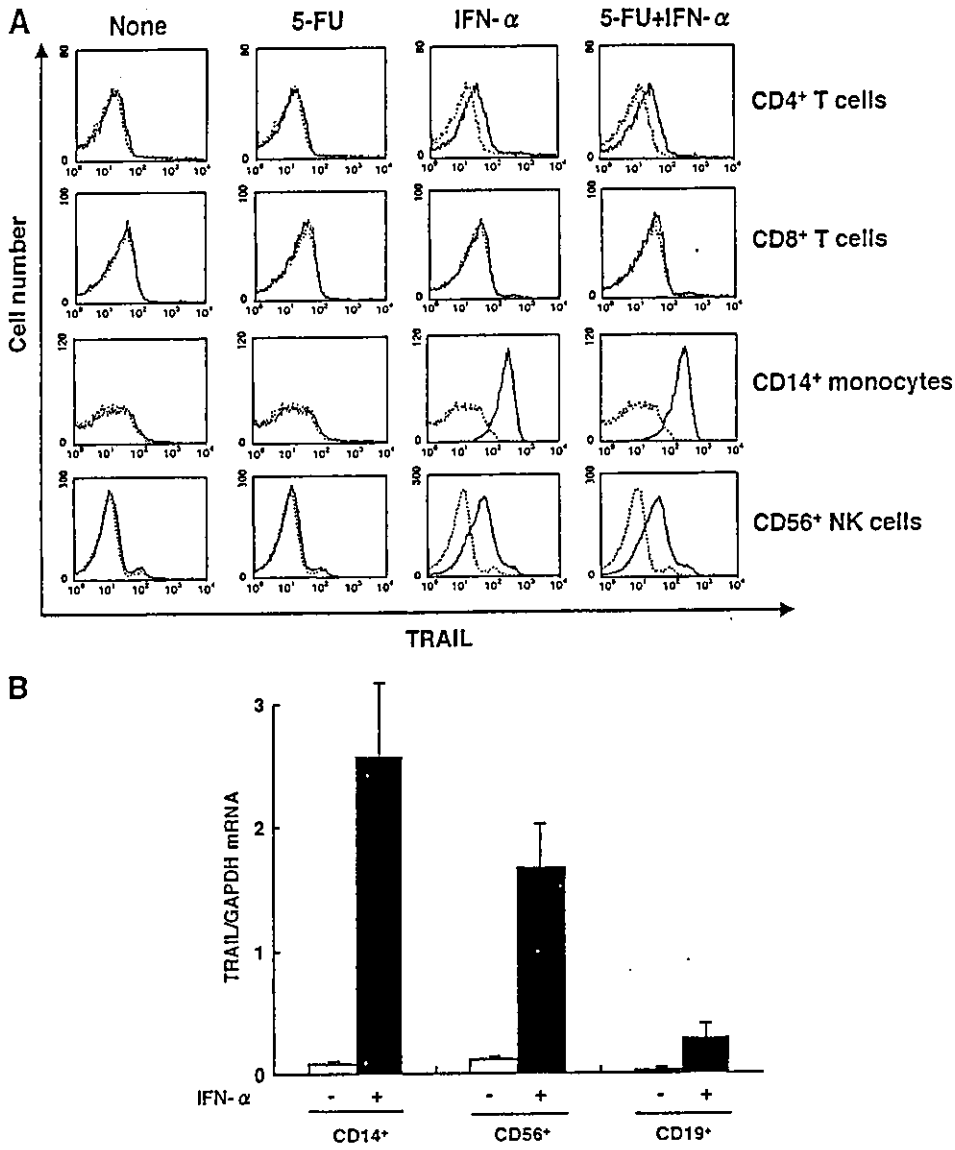

Fig. 3 *A*, regulation of TRAIL expression on $CD4^+$ T cells, $CD8^+$ T cells, $CD14^+$ monocytes, and $CD56^+$ NK cells in PBMC by 5-FU and/or IFNα. PBMC from healthy subjects were cultured in the presence or absence of 5-FU (0.5 μg/mL) and/or IFNα (500 units/mL) for 24 hours and then stained with biotinylated anti-TRAIL mAb followed by phycoerythrin-labeled avidin and FITC-labeled antihuman CD4, CD8, CD14, or CD56 mAb. *Dotted lines*, staining with biotinylated control IgG; *solid lines*, staining with biotinylated anti-TRAIL mAb. Similar results were obtained in three independent experiments. *B*, TRAIL mRNA expression in $CD14^+$ monocytes, $CD56^+$ NK cells, and $CD19^+$ B cells. Cells were isolated from PBMC by using anti-CD14, anti-CD56, and anti-CD19 immunomagnetic beads and Magnetic Cell Sorting and cultured in the presence (*closed bars*) or absence (*open bars*) of IFNα (500 units/mL) for 24 hours. LightCycler PCR and detection system were used to do quantitative RT-PCR for TRAIL, and expression of TRAIL mRNA is indicated relative to GAPDH. Data are mean ± SD of three independent experiments.

IFNα-stimulated PBMC cytotoxicity against untreated or 5-FU–treated HCC cell lines for which 5-FU and soluble TRAIL exhibited synergistic (HLF) or additive (HepG2) effect. We first used $CD4^+$ T cells, $CD8^+$ T cells, and $CD4^-CD8^-$ cells isolated from PBMC as the effector cells after incubation with or without IFNα for 24 hours. As shown in Fig. 4*A*, $CD4^-CD8^-$ cells, but not $CD4^+$ or $CD8^+$ T cells, were the main effector cells that exhibited substantial cytotoxicity against HLF and HepG2. When $CD4^-CD8^-$ cells were stimulated by IFNα, the cytotoxicity was significantly increased from 3.6 to 18% against HLF and from 43 to 63% against HepG2 at an E:T ratio of 20. Moreover, when the target cells were pretreated with 5-FU, IFNα enhanced the cytotoxicity of $CD4^-CD8^-$ cells from 19 to 54% against HLF and from 48 to 66% against HepG2. These results indicate a synergistic effect against HLF and an additive effect against HepG2 of the combination of IFNα and 5-FU on $CD4^-CD8^-$ cell-mediated cytotoxicity.

To investigate which subset of $CD4^-CD8^-$ cells was responsible for the IFNα-induced cytotoxicity, we prepared effector cells that were depleted of $CD14^+$ monocytes and/or $CD56^+$ NK cells from $CD4^-CD8^-$ cells. As shown in Fig. 4*B*, $CD4^-CD8^-CD14^-$ cells (mainly composed of NK cells and B cells) and $CD4^-CD8^-CD56^-$ cells (mainly composed of monocytes and B cells) exhibited higher cytotoxicity against HLF cells than $CD4^-CD8^-CD14^-CD56^-$ cells (mainly composed of B cells). IFNα significantly enhanced the cytotoxicity of $CD4^-CD8^-CD14^-$ cells, and pretreatment of the target cells with 5-FU significantly enhanced the cytotoxicity by both $CD4^-CD8^-CD14^-$ cells and $CD4^-CD8^-CD56^-$ cells. These results suggested that both $CD56^+$ NK cells and $CD14^+$ monocytes were the major effector cells that largely contributed to the IFNα-induced cytotoxicity of PBMC against 5-FU–treated HCC cells.

Finally, we examined the contribution of TRAIL by using